Applied Surface Science Advances 9 (2022) 100233

Contents lists available at ScienceDirect

Applied Surface Science Advances

journal homepage: www.sciencedirect.com/journal/applied-surface-science-advances

Anode materials for lithium-ion batteries: A review

P.U. Nzereogu [a], A.D. Omah [a,c], F.I. Ezema [b,c], E.I. Iwuoha [d], A.C. Nwanya [b,c,*]

[a] Department of Metallurgical and Materials Engineering, University of Nigeria, Nsukka, Nigeria
[b] Department of Physics and Astronomy, University of Nigeria, Nsukka, Nigeria
[c] African Center of Excellence, ACE-SPED, University of Nigeria, Nsukka, Nigeria
[d] DSI/NRF SARChI Chair for NanoElectrochemistry and Sensor Technology, Faculty of Sciences, University of the Western Cape, Bellville, Cape Town, South Africa

ARTICLE INFO

Keywords:
Anode material
Carbon
Lithium-ion battery
Silicon
Transition metal oxide

ABSTRACT

The need for eco-friendly and portable energy sources for application in electrical, electronic, automobile and even aerospace industries has led to an ever-increasing research and innovation in lithium-ion battery technology. Owing to the research and discoveries in recent years, lithium-ion batteries (LIBs) have stood out as the most suitable device for the storage of electrical power for application in mobile appliances and electric vehicles. This is as a result of the very attractive properties inherent in LIBs, which include lightweight, high energy density, small-scale size, few memory effects, long cycle life and low pollution. In this review article, recent advances in the development of anode materials for LIBs will be discussed, along with their advantages and disadvantages. New approaches for alleviating the drawbacks associated with LIB anode materials will also be highlighted.

1. Introduction

Diverse sources of energy and energy production techniques have been exploited over the years. The bulk of energy available to man is obtained from sources that are unfriendly to the environment and which pose certain levels of risk and danger to the health of man. Such sources include fossil fuel-based energy sources such as crude oil, natural gas, coal among others. Due to the increasingly more serious environmental threats posed by these sources of energy, an increased research effort has been recorded in recent years with regards to new and clean sources of energy, effective methods of energy conversion and techniques for energy storage. In the wake of these researches, many novel advancements and innovative developments have been recorded in diverse sources of clean energy. These sources include solar and wind energy. However, these new sources of renewable and environmentally friendly energy are not entirely free of challenges. The major challenge is that they do not provide an uninterrupted and continuous flow of power (electric energy). Hence, the need for energy storage devices with maximum efficiency and adequate storage capacity for application in the storage of the produced energy comes to the fore.

One of the first attempts at energy storage was the use of Lead-acid batteries. Lead-acid batteries possess a charge/discharge state that is commendably stable, but some of their major drawbacks are their bulky size and high weight, which makes them unfit for use in portable, light electric devices. The major requirements for an energy storage medium in electrical and electronic applications in recent years are lightweight, long life span, cyclability, high energy density and accelerated charging rate. Nickel-cadmium (Ni-Cd) and Nickel-metal hydride (Ni-MH) batteries are some of the earliest energy storage devices that found application in portable electronic equipment and devices(phones, digital cameras etc.). While the Ni-Cd battery exhibited great capacity when subjected to high currents, it however, showed adverse memory effects, which led to a significant decrease in battery life, along with alarming toxicity issues as a result of its components. Although the Ni-MH battery exhibited a longer life span and is eco-friendly, it faced the challenge of leakage. Hence, the lithium-ion battery (LIB) was innovated with high prospects.

The liquid leakage challenge posed by the conventional secondary batteries is conveniently solved by the solid polymer electrolyte in lithium-ion batteries. Secondly, in a lightweight architecture, its volume reduces to a compact size, meeting the requirements of portable devices [1]. In recent years, the power storage technology employed by a vast majority of laptops, mobile phones and other compact and light electronic facilities is the LIBs. However, even though the LIBs have gained very wide acceptance and deployment in various applications, it still cries for further research, innovations and developments. This is due to

* Corresponding author at: Department of Physics and Astronomy, University of Nigeria, Nsukka, Nigeria.
E-mail address: chinwe.nwanya@unn.edu.ng (A.C. Nwanya).

https://doi.org/10.1016/j.apsadv.2022.100233
Received 20 December 2021; Received in revised form 9 March 2022; Accepted 9 March 2022
Available online 27 March 2022

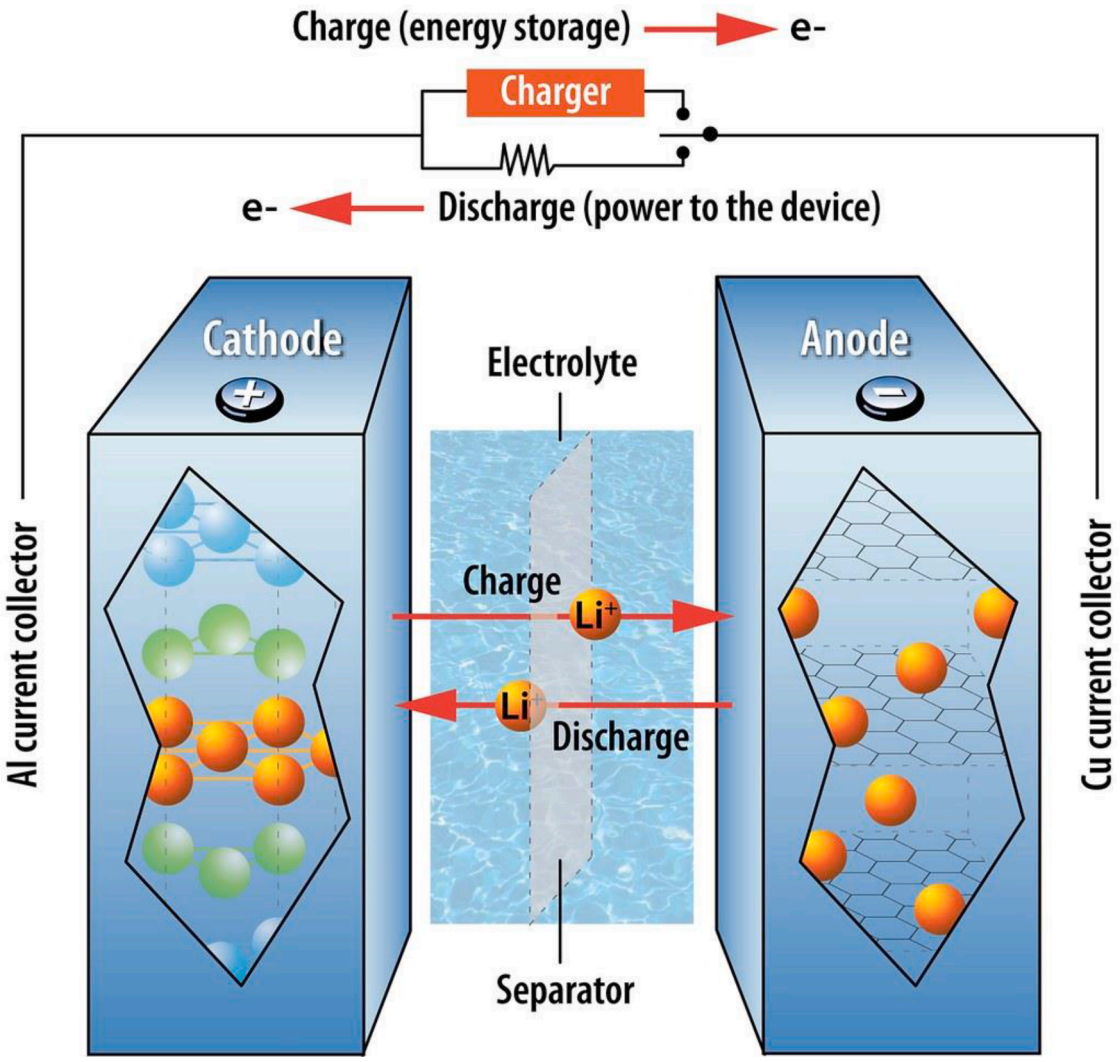

Fig. 1. A schematic diagram showing how a lithium-ion battery works. Credits: (Diagram by Argonne National Laboratory, licensed under CC BY-NC-SA 2.0)

the need for batteries with higher energy density, long battery lifespan, and high charging speed that will meet the energy requirements for extensive energy storage operations and utilization, (such as solar cells and electric vehicles) in the fast-growing and advancing electrical, electronics and automobile industries. In addition to this, the scope and applications of LIBs have been expanded with the innovation of technological products such as electric-powered automobiles (that is, the EVs and HEVs, which stand for electric vehicles and hybrid electric vehicles, respectively). The power source in an electric-powered automobile is the rechargeable battery. A motor, which is one of the components of the vehicle's engine, will then convert the electrical energy supplied by the battery into mechanical energy. To say the least, the advent and popularity of technological products such as solar cells, EVs and HEVs, which are a great step to the establishment of an eco-friendly society, have made the study and research on improving the properties, and hence the performance of LIBs very necessary, crucial and critical.

2. The concept of lithium-ion batteries

A lithium-ion battery, as the name implies, is a type of rechargeable battery that stores and discharges energy by the motion or movement of lithium ions between two electrodes with opposite polarity called the cathode and the anode through an electrolyte. This continuous movement of lithium ions from the anode to the cathode and vice versa is critical to the function of a lithium-ion battery. The anode, also known as the negatively charged electrode, discharges lithium ions into the electrolyte as shown in Fig. 1. The discharged ions are subsequently conveyed to the cathode, which is also referred to as the positively charged electrode, where they are absorbed. This, in a simple statement, is the process of energy discharge in LIBs. Similarly, during the charging process, there is a progressive migration of lithium ions from the cathode to the anode via the electrolyte [1]. From the foregoing, it is clear that the charging procedure is simply the exact opposite of the discharge process.

In recent years, lithium-ion batteries (LIBs) have gained very widespread interest in research and technological development fields as one of the most attractive energy storage devices in modern society as a result of their elevated energy density, high durability or lifetime, and eco-friendly nature. They have also been established as the most competent sources of power for mobile, flexible and wearable electronic appliances, gadgets and devices, which include mobile phones, laptops, and digital cameras, owing to their attractive qualities when contrasted with other types of batteries, like the alkaline batteries and conventional Ni- MH or Ni-Cd batteries. In fact, LIBs are currently being considered as the power sources of choice for applications involving large-scale energy storage, such as solar cells, electric vehicles, among others. One important fact is that the electrodes' quality has anoutstanding effect on the efficiency and performance of a LIB. This implies that any innovation leading to an enhancement in the capacity of the electrodes would generally improve the overall quality and efficiency of the battery, both

in its energy density, cyclability, and lifespan. This may ultimately lead to the full deployment of LIBs in electric-powered automobiles (EVs and HEVs) and other energy storage applicationsbothin large-scale and small-scale.

The anode is a very vital element of the rechargeable battery and, based on its properties and morphology, it has a remarkable effect on the overall performance of the whole battery. As it stands, due to its unique hierarchical structure, graphite serves as the material used inmost of the commercially available anodes. Once lithium ions embed into graphite, the fairly large interstice between two adjoining layers of carbon atoms offers insertion sites for the lithium ions, thereby preventing the anode material's shape, size, and structure from changing during the charge-discharge process [2]. Aside from this conventional mode of lithium-ion interactions, other novel mechanisms have also been explored. Such mechanisms include the redox reactions in transition metal oxide anodes and the displacement reaction in alloy anodes.

Certain parameters are prioritized in LIB studies with a view to quantifying and evaluating the performance of the batteries. These include the rate capacity, coulombic efficiency and reversible/irreversible capacity. In earlier studies, it was thought that the outstanding rechargeable characteristics of LIBs were due to the reversible recycling of lithium ions, but in effect, numerous losses take place inevitably in the actual intercalation/de-intercalation cycle [3]. One of the major losses occurs as a result of the creation of a layer called Solid Electrolyte Interface (SEI). This occurs during the first charge-discharge phase and is the outcome of the reaction between the electrolyte and the electrode material. SEI, on one hand, is not entirely adverse to the operation of LIBs, since it aids in ensuring the freedom of movement for the lithium ions while restricting the embedding of the solvent into the electrode. On the other hand, because SEI formation leads to the depletion of several lithium ions from the system and SEI layers inevitably result in an irreversible capacity loss in batteries, radical measures must be employed to at least limit or assuage the loss of reversible capacity in LIBs.

The coulombic efficiency is another important parameter considered in LIBs architectural design. Coulombic efficiency is the ratio of lithium extraction capacity to lithium penetration capacity in the same cycle. This simply means the ratio of lithium charging capacity to the discharging capacity for the cathode material and vice versa for the anode material. Coulombic efficiency can be reduced by electrolyte decomposition and chemical or physical variations in electrode active materials. LIB capacity varies depending on the current. High capacity is typically obtained at low currents; thus, discharge capacity at high currents, also known as rate capacity, becomes an important factor to consider [4]. It is worthy of note that when lithium-ion batteries are charged and/or discharged excessively it will have an irreversible damaging effect on the cathode and anode. In practice, power density is an important factor to consider in addition to volumetric capacity and specific capacity. According to reports, reducing the thickness of the electrodes to the barest minimum may serve as a very potent and efficient step in increasing the power density of the battery while decreasing both current density and resistance [5]. Furthermore, improving manufacturing technology and efficiency of production is critical to meeting the growing market demand for mobile, lightweight, and small electric and electronic products.

It is generally believed that breakthroughs in LIB technology would require innovative chemistries for both the electrode and electrolyte components. The aim of the entire initiative is thus to identify, 'doctor' and deploy materials having capacities and performances higher than those offered by the anode and the cathode used in conventional types. Hence, the objective of this review is to report the innovations and advancements in developing new anode materials as a possible replacement for graphite in LIBs. This review discusses four broad categories of anode materials used in the development of high-performance LIBs, viz: (i.) Alloy Materials, (ii.)Conversion type Transition-Metal Compounds, (iii.) Silicon-based Compounds, and (iv.) Carbon-based Compounds. In addition, the different bottlenecks associated with and preventing the full integration of these anode materials in commercial LIBs and possible solutions are mentioned in the review.

3. Anode materials

In the preceding section, it was clearly stated that the nature and properties of the anode material are cardinal to the overall battery performance. The capacity and performance of the battery not only depends largely on the intrinsic characteristics of the anode material but also on its morphology. Consequently, the suitable and appropriate structural design employed is much more important than the material selected. Many high-performance anode materials have been explored as novel materials for the next generation of LIBs. Among them are alloy materials, conversion-type transition metal compounds, silicon-based compounds, and carbon-based compounds.

3.1. Alloy material

It is common knowledge that graphite anodes have the problem of poor capacity and are associated with safety concerns. To correct these deficiencies, alloy anodes (such as Aluminum (Al), Tin (Sn), Magnesium (Mg), Silver (Ag), Antimony (Sb), and their alloys) are used. Alloy anodes are known to have a specific capacity that is two to ten times higher than that of anodes made of carbon material. Also, alloy anodes like Tin (Sn) alloys have higher onset voltage above Li/Li^+ which can help prevent lithium deposition, which is common in graphite anodes [6]. Furthermore, alloy anodes offer outstanding processing qualities and a high charge-discharge capacity. All these factors combine to make alloy anodes an intriguing topic with potential for LIB advancement. To add to this, there is also a concept in the field of alloy anodes known as alloy negative materials. They are simply metals with high purity or multi-component alloys which possess a significant storage capacity for lithium ions.

The underlying concepts of metal anode conduction center on the insertion process. Another relevant concept also is the chemical reaction. Here lithium ions react with the active metal to generate a Li_nM compound (M represents metal). n has a value greater than one. This is the major explanation for the high potential lithium capacity of alloy anodes, which is significantly greater than that of carbon anodes. Notwithstanding, alloy anodes have some associated drawbacks. According to reports, the massive volumetric expansions caused by the creation of a new phase severely compromises LIB characteristics [7]. Again, disadvantages such as poor electrical conductivity plus the substantial variations in the material's volume in the process of insertion/extraction of lithium ions result in issues such as substantial irreversible capacity loss during the first cycle and rapid capacity loss in subsequent cycles. These performance issues can be attributed to some inherent electrochemical mechanisms in the alloy materials. Some of these mechanisms are listed thus:

(a) Because of oxygen's low atomic weight, significant quantities of lithium can react with very tiny amounts of O_2 to form a layer of lithium oxide of very small thickness which will deposit on the metal's or alloy material's surface. This leads to Li loss, and consequently, an irreversible loss of capacity.
(b) Alloy anodes experience low lithium-ion diffusion rates leading to the trapping of Li ions within them, hence making the otherwise reversible lithiation/de-lithiation process somewhat irreversible. These events also result in the production of unwanted compounds of lithium or the adsorption of Li ions on atoms located at the structural defects sites in the metal resulting in permanent capacity loss.
(c) The SEI film in alloy anode comprises of lithium oxalates, $ROCO_2Li$, Li_2CO_3, and sometimes also includes a ROLi mixture. Contrary to what is observed in LIB anodes made of graphite, the

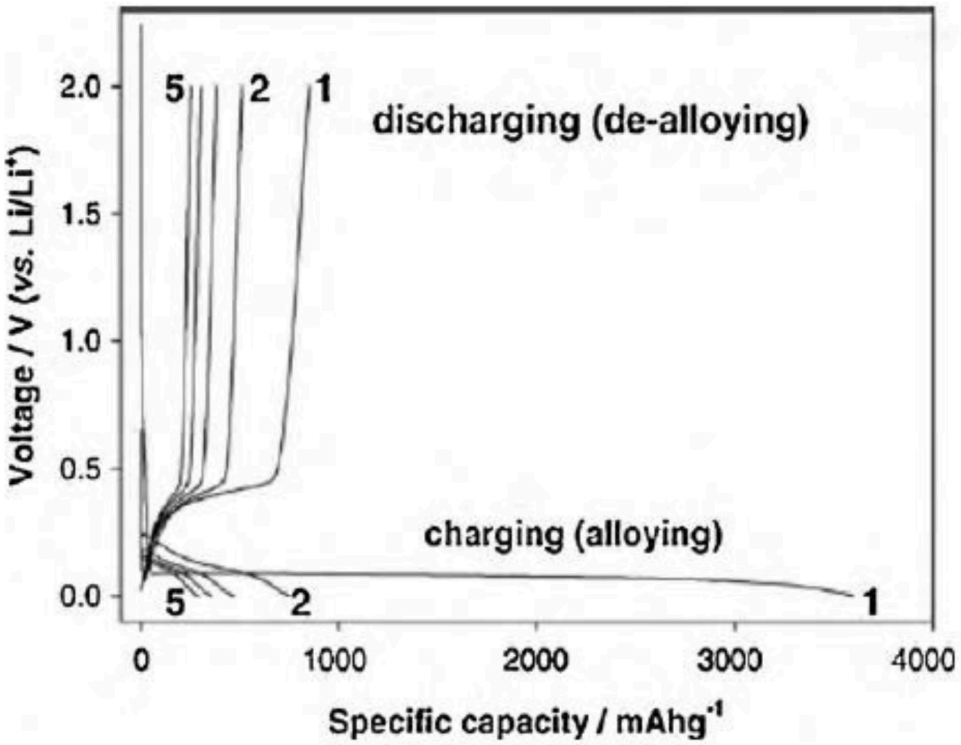

Fig. 2. Charge–discharge voltage profiles of a pure silicon anode with an average powder size of 10 μm. Reproduced from [10] with permission.

solid electrolyte interface films developing on the surface of alloy anodes experience a rupture and regeneration process because of the volume expansion and compression. Increasing the amount of Li_2CO_3 present in the film as the process of cycling progresses will change the chemical composition of the alloy. The thickness of the SEI films increases as the process continues and salt-degradation products build up. This ultimately decreases both the efficiency of the initial cycle and subsequent capacity.

(d) Because of the dramatic volume changes in the cycling process, the active material and the current collector become electrically disconnected. This occurs more often when lithium ions are delithiated from the electrode.

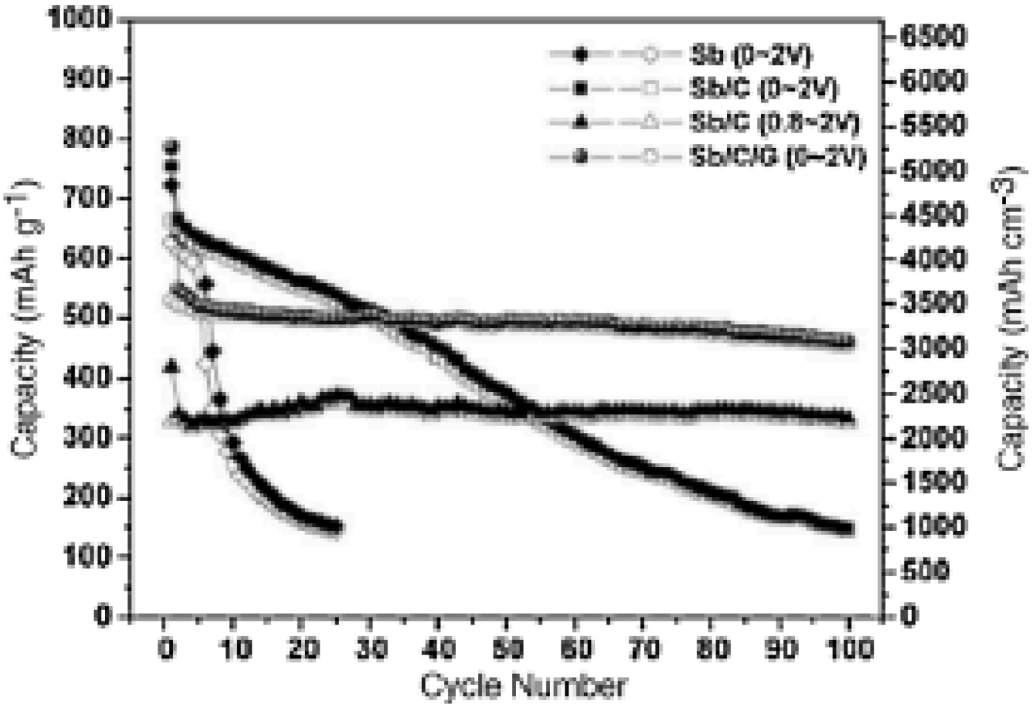

Fig. 3. comparison of cycle performance for Sb, Sb/carbon and Sb/carbon/graphite nanocomposites under different voltage windows. Reproduced with permission from [14].

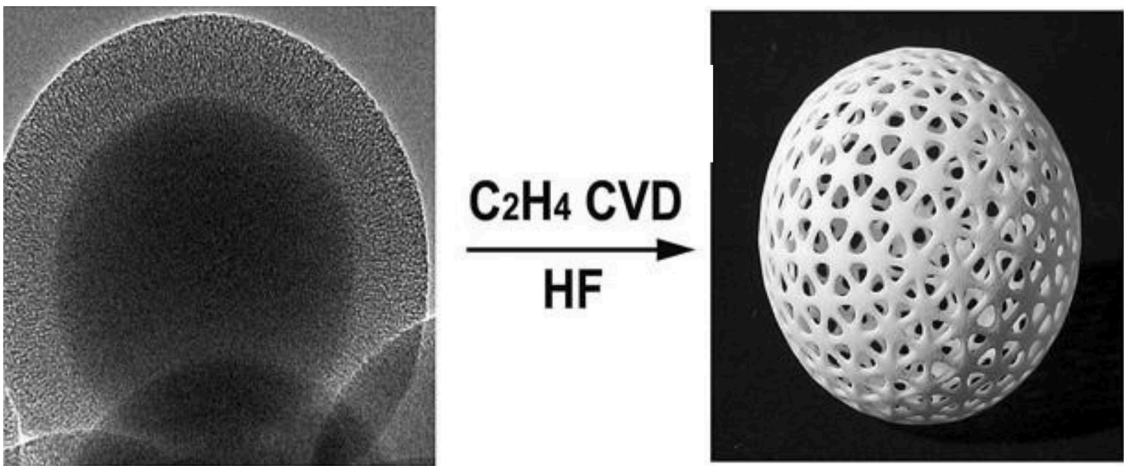

Fig. 4. Diagram showing hollow mesoporous carbon spheres [reproduced from Ref [17]. under the terms and conditions of the Creative Commons Attribution 3.0 Unported (CC BY 3.0) licence].

Two fundamental needs for improved anode materials are low irreversible capacity and long cycle life. Regrettably, early research discovered that many alloy anodes have large initial irreversible capacities (the difference between charge and discharge capacity) and fast capacity fading during cycling (reversible capacity loss) [8,9] Fig. 2.. depicts a charge/discharge curve for Si alloy anodes [10]. At the first cycle, it is clear that the delithiation capacity (charge) is substantially smaller than the lithiation (discharge) capacity.

The irreversible capacity loss after the first cycle is quite substantial (2650 $mAhg^{-1}$), and the coulombic efficiency is poor (just 25%). In addition, the capacity fell rapidly throughout the subsequent cycles; after five cycles, the reversible capacity had plummeted by 70%. This sort of action has been observed frequently in different alloy systems [11,12], and the electrochemical mechanisms already mentioned above are thought to be the causes of high irreversible capacity in alloy anodes

Some of these aforelisted challenges can be cushioned by techniques that modify the alloy surface in order to check the apparent loss of capacity. For instance, depositing a thin layer that will serve as a shield on the nano-alloy particles' surface can easily prevent oxidation of the anode and its aggregation [13]. Furthermore, carbon's superior capacity can be used to make up for the inadequacy of alloy electrodes. Developing high-conductivity graphite, with a layered pattern, which will serve as a dispersant or substrate for alloy anodes, for example, can significantly reduce the loss of capacity. In comparison to carbon-shelled pure tin anodes, it has been shown from previous studies that the carbon shell ultimately extends the lifespan of the battery and generates better potential between Li/Li^{+}. Higher carbon content generally results in greater capacity retention, but at the price of lower specific capacity and increased irreversible capacity loss. Carbon-composite anodes' first-cycle irreversible capacity is greatly influenced by the carbon type and preparation procedure, as stated in Section 3.4. In addition to particle size control, numerous carbon nanocomposites demonstrated stable cycle lifetimes of more than 100 cycles Fig. 3. illustrates an example of how the inclusion of carbon (C) and graphite (G) increased the cycle life of a nanocrystalline Sb anode [14].

Numerous carbon structures and compositions have been utilized for the above-mentioned technique, some of which are carbon fibres, carbon nanotubes, hollow carbon spheres, carbon coating layers, etc., each with its own set of advantages and disadvantages [15]. To buttress this, the studies of Zhang et al [16]. come in handy. Zhang et al. produced TNHCs (these are tin nanoparticles whose diameter is below 100 nm encased in a hollow carbon sphere shell whose diameter is close to 20 nm) to be used as an anode material. The morphology and shape of the hollow carbon sphere shell, as shown in Fig. 4, make room for a healthy expansion of the tin nanoparticles without the electrical disconnection of the active material from the current collector.

This resultant anode has a cycling retention of over 800 $mAhg^{-1}$, which after 100 cycles still maintained more than 500 $mAhg^{-1}$. It also exhibited a good working potential. The observation after various researches clearly shows that the amount of graphite present is directly proportional to the secondary battery life. However, there was also a marked decline in specific capacity and an increase in irreversible capacity loss.

Alloy electrodes have, in recent times, demonstrated improved electrochemical efficiency for advanced LIBs. In the case of the unreactive shell, an amorphous Tin–Calcium alloy was produced using a solution technique that takes advantage of the reducingpropertyof $NaBH_4$, and it appears in the shape of Li_5Sn_2 crystallite with the Calcium shell in the process of lithiation/delithiation. Reddy and Varadaraju [18] created a LIB anode using an $NbSb_2$ alloy in which antimony reacts with lithium yielding Li_3Sb. Here niobium does the work of a buffer substrate. The output and efficiency of the battery are improved as a result of the stress release and reduction in volume variations. Yin et al [19]. produced an Ag–Sn alloy ($Ag_{52}Sn_{48}$ and $Ag_{46}Sn_{54}$), which shows a reversible capacity of 800 $mAhg^{-1}$ to be used as an anode. In this setup, Ag serves as an unreactive matrix with buffer action. Mao and Dahn [20] produced an alloy powder of Sn–Fe–C. In this alloy, $SnFe_3C$ acts as the inert matrix, while Sn_2Fe is the active phase. From their work, when the composite is made with Sn_2Fe and $SnFe_3C$ with compositions of 25% and 75%, respectively, the battery exhibits elevated reversible capacities near 1600 mAh cm^{-3} and an excellent cyclability.

3.2. *The conversion-type anode materials*

From the findings of Lu et al [21]., conversion-type transition-metal compounds (CTAM) have risen to prominence as highly promising anode materials for lithium-ion batteries. This is as a result of their numerous attractive compositions alongside a high theoretical specific capacity. Some examples of conversion-type anode materials (CTAMs) in LIBs include transition-metal sulphides, oxides, phosphides, nitrides, fluorides, and selenides. One of the advantages is that when compared to alloy anode materials their production costs could be relatively on the lower side. This is consequent to the fact that many CTAMs appear in their natural forms. Very good examples are magnetite (Fe_3O_4), pyrite (FeS_2), and pyrolusite (MnO_2). Secondly, as a result of their lower lithium-intercalation potential CTAMs, unlike graphite anodes, do not experience the formation of lithium dendrites and therefore may make provision for better safety of operation for the LIB. Notwithstanding, CTAMs have some major drawbacks, which include inherent poor electronic and ionic conductivity, continuous electrolyte decomposition,

Fig. 5. Diagram showing the fabrication process for YDS-FCCNs. [Reprinted with permission from Ref [22]., Copyright (2020), Elsevier]

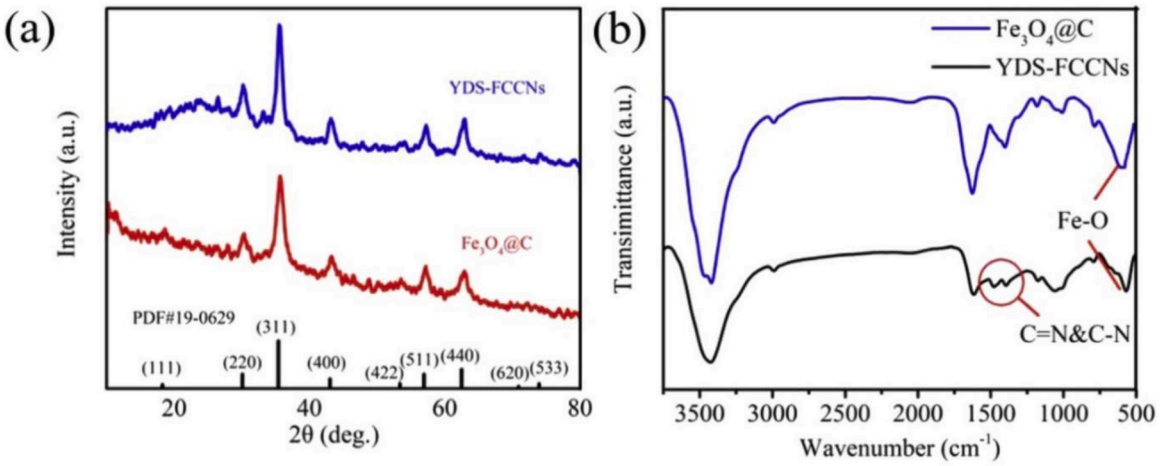

Fig. 6. (a) XRD representation of Fe_3O_4@C and YDS-FCCNs. (b) FT-IR spectra of Fe_3O_4@C and YDS-FCCNs. [Reprinted with permission from Ref [22]., Copyright (2020), Elsevier]

and relatively large volume expansion (<200%). However, technological progress has been recorded over the years using nano-engineering techniques to increase the capacity of CTAMs for lithium storage. Some examples of Conversion-type Transition-metal Compounds are discussed in details in the next sections:

3.2.1. Transition metal oxides

Transition metal oxides (MO_x, where M = transition metals which include iron, cobalt, nickel, copper, and zinc) possess some attractive characteristics which have made them generate a lot of interest as top candidates for LIB anode materials. They are non-toxic, possess high power density, theoretical specific capacity, are abundant in nature and have a low-cost fabrication process. One good case study is iron oxide materials (e.g., Fe_3O_4), which have lately gained increased recognition as potential anode material due to their elevated theoretical capacity (~926 $mAhg^{-1}$). However, the so-called attractive iron oxide materials still have their drawbacks. They display a rapid capacity decrease and poor cycling stability. This is attributed to the pulverization of the active materials during the charge/discharge process. In addition, when compared to graphite, Fe_3O_4 exhibits poor electron conductivity. This results in an eventual poor rate performance.

In a bid to allay the drawbacks in the structural stability and the electrical conductivity of Fe_3O_4- based anode materials, Zang et al [16]. designed and synthesized what is known as yolk-double shell Fe_3O_4@C@C nanospheres (YDS-FCCNs) as shown in Fig. 5. The process involves synthesizing Fe_3O_4@C nanoparticles from ferrocene using a solvothermal method (one-pot synthesis). The as-obtained Fe_3O_4@C is subsequently coated with a layer of SiO_2 by TEOS hydrolysis. This is followed by a uniform coating of the outermost part with a layer of polydopamine, after which it is calcined in a tube furnace filled with argon in a process called carbonization. To obtain the YDS-FCCN, the SiO_2 layer of the carbonized product is etched selectively with the aid of a NaOH solution. From their findings, the YDS-FCCNs exhibited an increased electrical conductivity as a result of the non-pulverization of the active materials along with improved lithium-ion transport. YDS-FCCNs gave a reversible specific capacity of 780 $mAhg^{-1}$ at 0.5 Ag^{-1} after 500 cycles as a LIB anode. The XRD patterns of nanoFe_3O_4@C and YDS-FCCNs, shown in Fig. 6a., shows consistency with the standard XRD pattern for magnetic Fe_3O_4. This confirms the crystal structure and composition of produced material. The FTIR spectra of YDS-FCCNs and Fe_3O_4@C in Fig. 6b, shows a characteristic peak at about 569 cm^{-1}, which relates to the vibrational stretch of Fe-O bonds. Compared with commercial nano Fe_3O_4 and Fe_3O_4@C, the YDS-FCCNs composite demonstrated good cycling stability and excellent reversible capacity. The novel double carbon shell structure showed enormous prospectsin improving the structural stability of other electrode materials [22].

Furthermore, Oh et al. [23] worked on improving the flexibility and efficiency of transition metal oxides (iron oxides) by interconnecting

them with carbon nanotubes. They modified the carbon nanotubes by attaching carboxyl groups to them with the aid of a HNO_3 solution. They also hydrolyzed polyacrylonitrile to form sulfonated polyacrylamide. The result was a sheet of hybrid nanofibres having the shape of a thorn bush which were deeply interconnected and integrated. These can serve as free-standing anodes for application in lithium polymer batteries that are highly flexible. The nanofibers comprised of α-Fe_2O_3 nanoparticles decorated carbon nanotubes. The as-produced HI-CNT/Fe_2O_3 were eventually fabricated in sheet form, in order to employ it as a self-supported anode. The polyimide matrix was also produced to serve as a freestanding gel polymer electrolyte for the flexible battery using the electrospinning process. From the observed results, the polyimide matrix has a porous structure that is finely connected, which enhanced the absorption of the electrolyte leading to high ionic conductivity [23,24]. A discharge capacity of 651 $mAhg^{-1}$ was recorded for a free-standing HI-CNT/Fe_2O_3 nanofiber anode after 100 cycles at a current density of 100 mAg^{-1}. To evaluate the specific capacity retention of the nanofibers, a full flexible cell comprising of the nanofiber anode and a $LiFePO_4$ cathode was set up. The specific capacity of the energy storage device, which was initially 148.9 $mAhg^{-1}$ before twisting, recorded a slight variation at 148.5 $mAhg^{-1}$ after twisting for 10 cycles. The morphology of the nanofibers recorded at the end of 100 cycles indicated that HI-CNT/Fe_2O_3 nanofibers maintained their original morphologies well after numerous cycling. Their exceptional structure can withstand extreme volume fluctuations of α-Fe_2O_3, thereby achieving higher structural stability for the HI-CNT/Fe_2O_3 nanofibers and ultimately resulting in an enhanced Li-ion storage property [25–27].

Other types of conversion-type transition metal compounds which have attracted significant research and developments as possible competitive alternatives employed as anode materials for lithium-ion batteries include the following:

3.2.2. Transition metal chalcogenides

The transition metal compounds that fall under this category include tin sulphide(SnS), molybdenum disulfide (MoS_2), iron disulfide (FeS_2), and cobalt sulfide (CoS_2). Chalcogenides have stood out as attractive anode materials whose theoretical capacity is quite high [28]. This is due to their Li (and Na) ions storage capacity by the mechanism of electrochemical conversion [29]. To further improve the cycling stability and rate performance of the chalcogenides (especially cobalt sulfide), which are hampered by significant alterations in the bulk dimensions of the material during charging/discharging, highly conductive and stable materials like polyaniline and graphene are applied as coatings on the surface of the sulfides [30,31].

3.2.3. Transition metal oxalates (TMOxs)

Transition metal oxalates are one of the most promising new anodes that have attracted the attention of researchers in recent years. They stand as a much better replacement for graphite as anode materials in future lithium-ion battery productions due to the exceptional progress recorded by researchers in their electrochemical properties [32,33]. Such compounds include zinc oxalates (ZnC_2O_4), cobalt oxalates (CoC_2O_4), manganese oxalates (MnC_2O_4), nickel oxalates (NiC_2O_4) and iron oxalates (FeC_2O_4). These compounds, however, also encounter huge volume expansions during li-ion insertion/extraction leading to low cycling performance. According to research, it has been observed that modifications in the particle size, structure and/or morphology of the materials will go a long way to arresting this challenge [34].

3.2.4. Transition metal carbides and nitrides (MXenes)

The transition metal compounds within the family of MXenes are titanium carbide ($Ti_3C_2T_x$) Mxene and selenides such as CoSe, $FeSe_2$ and $NiSe_2$. $Ti_3C_2T_x$ as a new anode material for LIBs has risen to a high standing consequent to its elevated electrical conductivity along with an outstanding chemical stability and a reduced lithium-ion diffusion impedance [35]. Its commercialization is however limited by its inherent low capacity and restacking characteristics [36,37]. To allay these drawbacks, the integration of high theoretical capacity transition metal oxides (such as Fe_3O_4) into the layers of $Ti_3C_2T_x$ to form hybrids with increased capacity for li-ion storage has been successfully experimented [38]. To further improve the electrochemical performance of the $Ti_3C_2T_x$, the number of its layers can be reduced, as it is observed that the higher the number of layers present, the more the possibility of some active layers in the internal surface of the $Ti_3C_2T_x$ being neglected from $Fe3O_4$ loading as a result of the multi-levelled nature of the $Ti_3C_2T_x$M-Xenes [38]. In addition to this, mixing the $Ti_3C_2T_x$ MXene with a transition metal selenide ($Co_{0.85}Se$ clad with carbon) to form hybrids has led to the fabrication of anode materials with exceptional volumetric stability, high electrical conductivity and a reversible capacity up to 700 $mAhg^{-1}$ [39].

Recent research has demonstrated that MXenes, due to its unique qualities such as layered structure, good electrical conductivity, and hydrophilicity, can be employed as anode materials for Li-ion batteries (LIBs) [40]. MXenes have been proven to have a high specific capacity value of 320 mAh/g at a current of 100 mA/g after 760 cycles. However, MXenes in general suffer from restacking during cycle, limiting their Li-ion storage potential. The majority of the research has concentrated on the Li-ion storage potential of multi-layered MXene, although they suffer from restacking during cycle and perform similarly to graphite [40]. According to the results of the investigations, increasing the interlayer spacing, altering the functional groups of MXenes, and synthesizing few-layered MXenes are the most essential strategies to improve MXenes' Li-ion storage capabilities. MXene-based composites are often manufactured with two goals in mind: limiting MXene restacking and buffering the volumetric expansion and loss of electrical contact of high-capacity anode materials, resulting in a synergistic effect between the MXenes and other composite ingredients. The findings of the examined studies show that adding modest concentrations of MXenes to metal oxides, transition metal dichalcogenides (TMDs), and silicon can greatly alleviate their difficulties for practical applications in LIBs [40].

3.2.5. Aluminium niobates

Aluminum niobates have emerged as a better alternative to the traditional titanium niobates ($TiNb_2O_7$ and$Ti_2Nb_{10}O_{29}$) to serve as an improved anode material for LIBs [41]. This is because despite their attractively high theoretical capacity and impressive electrochemical properties titanium niobates possess a poor charge conductivity due to their reduced rate capability [42,43].

3.2.6. Transition metal phosphides

The phosphides of importance in this category include tin, cobalt, copper, nickel and iron phosphides and their respective composites. As a result of their metallic features, increased thermal stability, exceptional specific capacity and safe operational potential, transition metal phosphides have attracted the attention of researchers as outstanding anode materials for lithium-ion batteries [44,45]. Nevertheless, their reduced inherent electronic conductivity and the cracking of the active materials caused by the huge volume fluctuations of phosphorus during the charging/discharging process pose a very high limitation to the electrochemical performance of the phosphides [38]. According to research, it has been observed that these drawbacks can be allayed by decreasing the particle sizes of the metal phosphides to nano-sized structures [46].

3.2.7. Binary transition metal oxides

Due to their high theoretical specific capacity, improved rate performance, and outstanding cycling stability, binary transition metal oxides have gotten a lot of attention as potential anode materials for lithium-ion batteries [47,48]. Compared to single transition metal oxides (such as Fe_2O_3, Co_3O_4, Mn_3O_4), binary transition metal oxides generally present improved electrochemical performance due to the synergistic effect of different metal elements [49]. Among transition

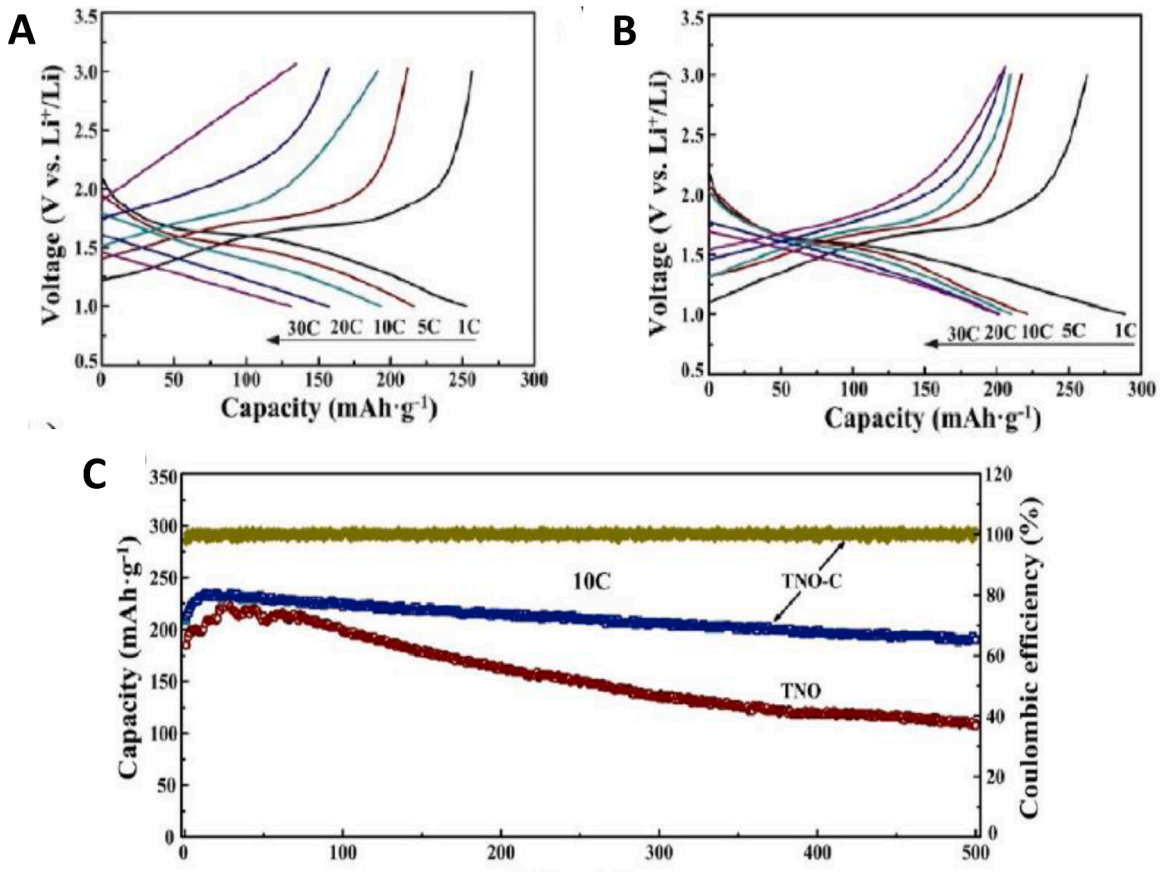

Fig. 7. Diagrams showing the Charge/discharge curves of the (a) pure $TiNb_2O_7$ and (b) $TiNb_2O_7$/C samples at different rates; and (c) long-term cyclic performance at 10 C, reproduced from Ref [63].

metal oxides, $ZnMn_2O_4$ offers various advantages, including environmental friendliness, low cost, and a substantially lower working voltage when compared to the Fe or Co -based oxides. With a lower charge voltage, the anode material can give a higher energy density. As a result, $ZnMn_2O_4$ has been proposed as a viable anode alternative for LIBs in place of conventional graphite [50]. To date, LIBs have been investigated using $ZnMn_2O_4$ nanomaterials as anodes in various morphologies, such as nanoflakes, nanowires, nanoparticles, and nanoflowers. By calcining a Zn–Mn citrate complex, Deng and Chen [51] were able to create agglomerated $ZnMn_2O_4$ nano-particles. At 200 mAg^{-1}, the nanoparticles had a specific capacity of 555 $mAhg^{-1}$ and 405 $mAhg^{-1}$ at 600 mAg^{-1}. For $ZnMn_2O_4$ nanowires, Kim et al. [52] reported a solid-state reaction of $Zn(Ac)_2$ with α-MnO_2 nanowires at a high temperature. After 40 cycles, the nanowires had reversible capacities of 450 $mAhg^{-1}$ at 500 mAg^{-1} and 350 $mAhg^{-1}$ at 1000 mAg^{-1}.

It is necessary to note that in spite of the outstanding features of transition metal oxides, their application in LIBs is generally limited by their low rated cycling performance owing to a very substantial change in volume during Li insertion/extraction. Furthermore, their applicability in LIBs is limited by their poor rate performance. To allay these, it has been observed that porous structures, could protect electrode integrity while also improving electrode structural stability due to their high tolerance for volume variation during discharge–charge cycles [53, 54]. If the porous structure can therefore be incorporated into one-dimensional nanomaterials, the resulting porous nanorods will benefit from both the porous nanostructure and the one-dimensional geometry. In LIBs, such a structure will most certainly perform well. Hence, Bai et al. [55] synthesized loaf-like $ZnMn_2O_4$ nanorods by annealing MnOOH nanorods and $Zn(OH)_2$ at 700 °C for 2 h. The obtained $ZnMn_2O_4$ maintained the one-dimensional shapeof the MnOOH nanorods and a pore-like structure was observed throughout the whole nanorod. For the production of loaf-like $ZnMn_2O_4$ nanorods, reaction time and temperatures are critical. $ZnMn_2O_4$ nanorods with poor crystallinity are formed when the reaction temperature is lower than 600 °C. When the reaction temperature is raised to 800 °C, $ZnMn_2O_4$ nanorods without porous features form. This is a highly typical occurrence in solid-state processes. Hence the optimal time and temperature for the synthesis is maintained at 700 °C for 2 h. The as-produced loaf-like $ZnMn_2O_4$ nanorods demonstrated a reversible specific capacity of 517 $mAhg^{-1}$ at a current densities of 500 mAg^{-1} after 100 cycles. The reversible capacity of the nanorods could still be retained at 457 $mAhg^{-1}$ even at 1000 mAg^{-1}. The loaf-like $ZnMn_2O_4$ nanorods' superior and improved electrochemical performances can be related to their one-dimensional shape and porous structure, which provide the electrode with efficient electron transport pathways and enough void spaces to tolerate volume change during the lithiation process [55].

Recently, intercalating titanium niobium oxide (TNO), which is another binary transition metal oxide anode material, with the general formula of $TiNb_xO_2$+2.5x, has received lots of attention as an alternative to graphite and $Li_4Ti_5O_{12}$ commercial anodes. The desirability of this family of compounds stems from their high theoretical capacities (377–402 mAh/g), high safety, high working voltage, excellent cycling stability, and significant pseudocapacitivebehavior [56]. However, the rate performance of TNO-based anodes is poor owing to their low electronic and ionic conductivities. TNO-based composites generally are prepared with the aims of enhancing the conductivity of TNO and achieving a synergic effect between the TNO and the other component of the composite. Compositing with carbon matrices, such as graphene and carbon nanotubes (CNTs) are the most studied strategy for improving the conductivity of TNO and optimizing its high-rate performance [56, 57].

Several kinds of titanium niobium oxide compounds with the general

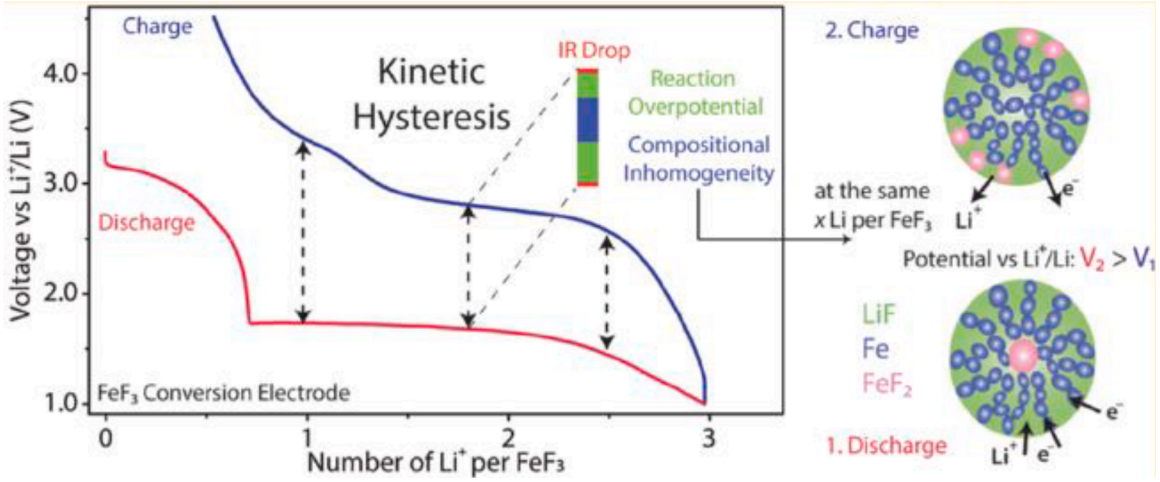

Fig 8. . Schematic diagram showing the large voltage hysteresis in FeF_3, a typical representative conversion material electrode. Reproduced from Ref [78]..

formula $TiNbxO_2$+2.5x have recently been presented as possible candidate materials for the anode of LIBs. By combining Spinel lithium titanium oxide (LTO) and niobium oxide (Nb_2O_5) in its novel architecture, these compounds not only have the advantages of LTO in terms of outstanding structural stability and a high working potential (1.0–2.0 V vs. Li/Li+) that prevents SEI formation, but they also have significantly higher theoretical capacity due to multiple redox couples of Ti^{4+}/Ti^{3+}, Nb^{5+}/Nb^{4+}, and Nb^{4+}/Nb^{3+}.

TNO has several benefits, however it has low electronic conductivity and weak ionic diffusivity, which results in a low rate capability. Overcoming these challenges will necessitate study in order to achieve the practical use of TNO. Doping [58], forming composites [59–61], and size refining [62] are the most successful ways for increasing the electrical conductivity of TNO. Composite creation is a simple and effective way for increasing the rate performance of TNO-based composites. The inclusion of extremely low levels of second phases with strong electrical/ionic conductivity, such as graphene and carbon nanotubes (CNTs), can greatly increase the rate performance of TNO anodes. Because carbon materials have excellent electrical conductivity, coating TNO anode materials with carbon (TNO/C) can increase electrochemical performance, particularly the rate capability of the battery. Yang et al [61]., for example, established a simple solvothermal process for producing carbon-coated porous $TiNb_2O_7$ microspheres Fig. 7. depicts the electrochemical performance of the generated samples. The $TiNb_2O_7$/C electrode demonstrated a discharge capacity of 200 mAh/g at 30 C, as shown in Fig. 7a and b, but the $TiNb_2O_7$ electrode provided only 132 mAh/g at the same rate. The cycle ability of the $TiNb_2O_7$/C sample, as shown in Fig. 7c, was 191 mAh/g after 500 cycles at 10 C with a capacity retention of 92%, but the $TiNb_2O_7$ anode had only 107.5 mAh/g with a capacity retention of 58.4%.

Aside from TNO-based composites with conductive reinforcements, the production of TNO with various types of anode materials might result in synergic benefits.

3.2.8. *Transition metal hydroxides*

Extensive research studies have been carried out on various transition metal oxides such as have been discussed above and many more, with interesting outcome in their electrochemical performances, rate capacities and cyclic stabilities [64,65]. It is, however, interesting to note that studies on corresponding metal hydroxides as anode for LIBs in the recent past are sparse, probably in apprehension of the OH group present in their framework, though $Ni(OH)_2$ has long found application in secondary alkaline batteries. Presently, however, this field of anode materials is gradually coming to limelight as researchers are picking interest in their diverse potentials. From literature, a number of studies are available wherein $Ni(OH)_2$ and Ni, Co mixed hydroxide have been used as anode materials in LIBs [66,67]. Specific capacity as high as 1416 $mAhg^{-1}$ has been reported with a composite of β-form of hexagonal $Ni(OH)_2$ nano flowers with a brucite like structure and multi-walled carbon nanotubes (MWCNTs), but with significant fading upon cycling, keeping just 30% of capacity after 50 cycles [66]. Li et al. [67] also showed good lithium storage properties (927 $mAhg^{-1}$) of β-Ni $(OH)_2$@reduced graphene oxide composite, but with low capacity retention (54.7% after 30 cycles). Ni et al [68]. demonstrated good cycle ability by hydrothermally developing $Ni(OH)_2$ directly on Ni foam; nevertheless, the material still had a poor cycle life when evaluated in powder form. A few investigations focused on the supercapacitive properties of metal hydroxides [69–71], with high specific capacitance values have been reported for layered mixed Co–Ni hydroxide nanocones (1580 Fg^{-1}) [69] and amorphous $Ni(OH)_2$ electrodes (2188 Fg^{-1}) [71]. These findings suggest that metal hydroxides have intriguing electrochemical characteristics and could be used as lithium battery anodes. Another interesting hydroxide material is $Cu(OH)_2$ whose features show promising potentials as effective alternative anode for LIBs. In a cage-like structure, $Cu(OH)_2$ has a layered framework with interlayered H-bonds [72,73]. Large interlayer spacing allows for quick Li^+ ion transfer/exchange while also increasing the effective active material–electrolyte interface area, which favors good intercalation properties. Pramanik et al [74]. investigated the electrochemical performance of chemically synthesized $Cu(OH)_2$ nanoflower arrays which was a 50 : 50 composite of $Cu(OH)_2$ and multiwalled carbon nanotubes (MWCNT). The resultant composite exhibited a reversible capacity of 522 $mAhg^{-1}$ at a current density of 0.1 mAcm- [2] with 95% retention of capacity after 50 cycles. The results prove that it can serve as a very competitive alternative in LIBs anodes over its corresponding oxides. Also these results for metal hydroxide anodes presented above are aimed at exciting researchers and stimulating renewed interest and further research into the viability of other metal hydroxides as alternative anodes for lithium-ion batteries.

3.2.9. *Large voltage hysteresis in CTAMs*

One major challenge observed in conversion type anode materials which grossly limits their large-scale application in LIBs despite their promising features is the unusually large voltage hysteresis between charge and discharge profiles as shown in Fig 8. At similar rates, the hysteresis of conversion electrode materials ranges from several hundred mV to 2 V [75], which is fairly similar to that of a Li-O_2 battery [76] but much larger than that of a Li-S battery (200–300 mV) [76] or a traditional intercalation electrode material (several tens mV) [77]. It results in a high level of round-trip energy inefficiency (less than 80%

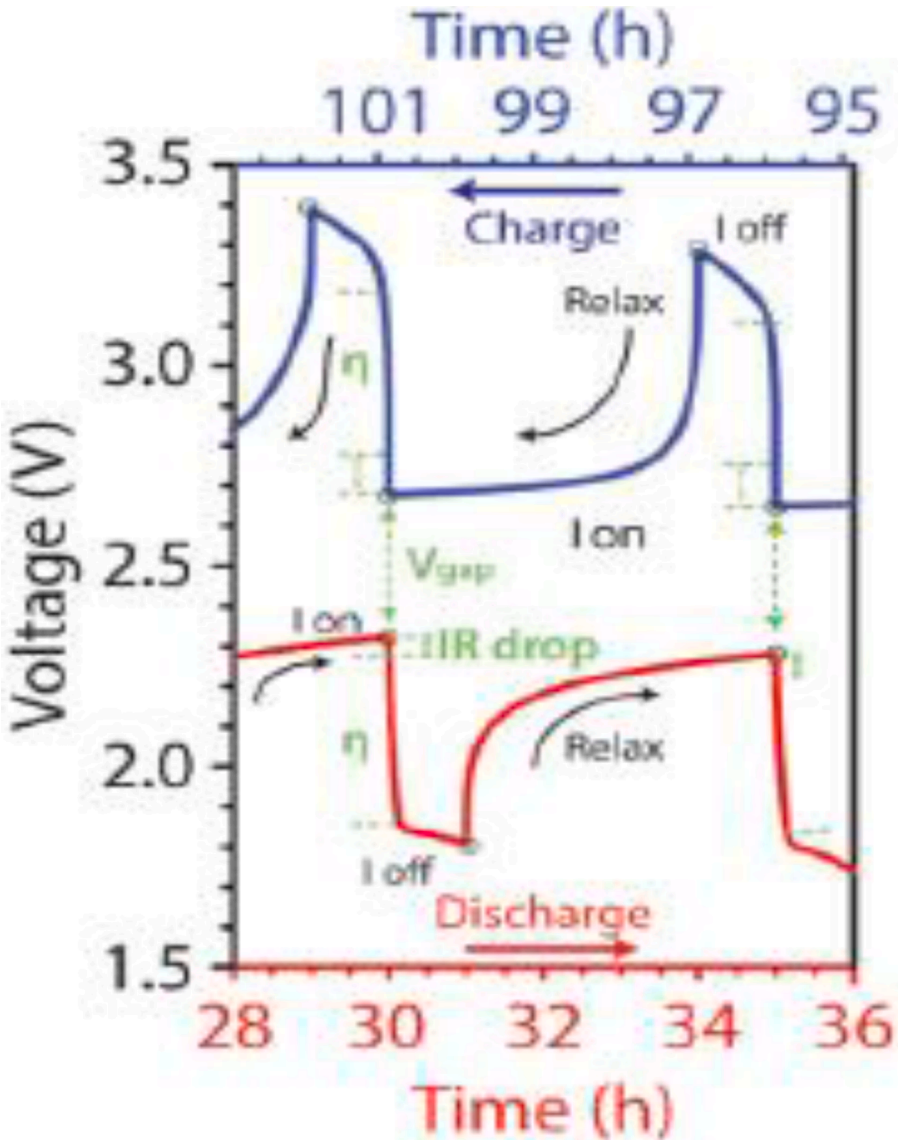

Fig. 9. A close-up view of the GITT curve for the electrode. IR drop, reaction overpotential (η), and the remaining voltage difference after relaxation (Vgap) are marked to show the components that contribute to the large voltage gap during cycling. Reproduced from Ref [78]..

energy efficiency), which is intolerable in practical applications.

To conquer this conundrum, it is essential to recognize the physical origins of the large voltage hysteresis, which have remained a mystery for many years. The current view is that a significant proportion of the voltage hysteresis is caused by asymmetric reaction pathways during discharge and charge, and that the presence of different intermediate phases leads to a significant split in electrochemical potential [79–81]. In a recent work, however, Li et al. [78] first correlated the voltage profile of iron fluoride (FeF_3), a typical conversion electrode material, with the evolution and spatial distribution of intermediate phases in the electrode using *in situ* X-ray absorption spectroscopy, density functional theory calculations, transmission electron microscopy, and galvanostatic intermittent titration technique (GITT). By combining all of their experimental and theoretical simulation results, the GITT concludes that the following components are the sources of the voltage hysteresis found at nonzero current, as illustrated in Fig. 9.

The first is the iR voltage drop, which is the abrupt voltage increase once the current is discontinued and is typically 100 mV in the tests. The second component is the reaction overpotential(η), which is necessary to nucleate and develop new phases, promote mass transfer, and overcome the interfacial penalty associated with the formation of nanophases. This overpotential is seen as a voltage drop when current is applied and a spike when current is withdrawn. The difference in spatial distribution of electrochemically active phases during discharge and charge, as well as the way these phases are connected in the electrochemical system (i.e., access to Li+ and electron), is the third component that leads to hysteresis, but has not been considered in detail in previous literature. This hysteresis due to compositional inhomogeneity cannot be completely abolished by voltage relaxation (zero current) since it is extremely difficult, if not impossible, to make the relevant phases (or Li^+ distribution), such as FeF_2 ("Li-poor" phase) and Fe/LiF ("Li-rich" phase), become spatially homogeneous solely by Li^+diffusion. This relaxation process also necessitates the migration of F and Fe^{2+} ions, which are normally quite sluggish.

These new insights propose techniques for reducing voltage hysteresis, which is critical for boosting battery energy efficiency. One simple way is to build a composite electrode out of nanostructured active particles size of which must be equivalent to the length scale of the conversion reaction (typically less than 10 nm for FeF_3) and which are directly coupled to electrically conductive scaffolds. Embedding active elements between graphene layers to create a graphite intercalation compound is one intriguing approach [82]. This is expected to reduce

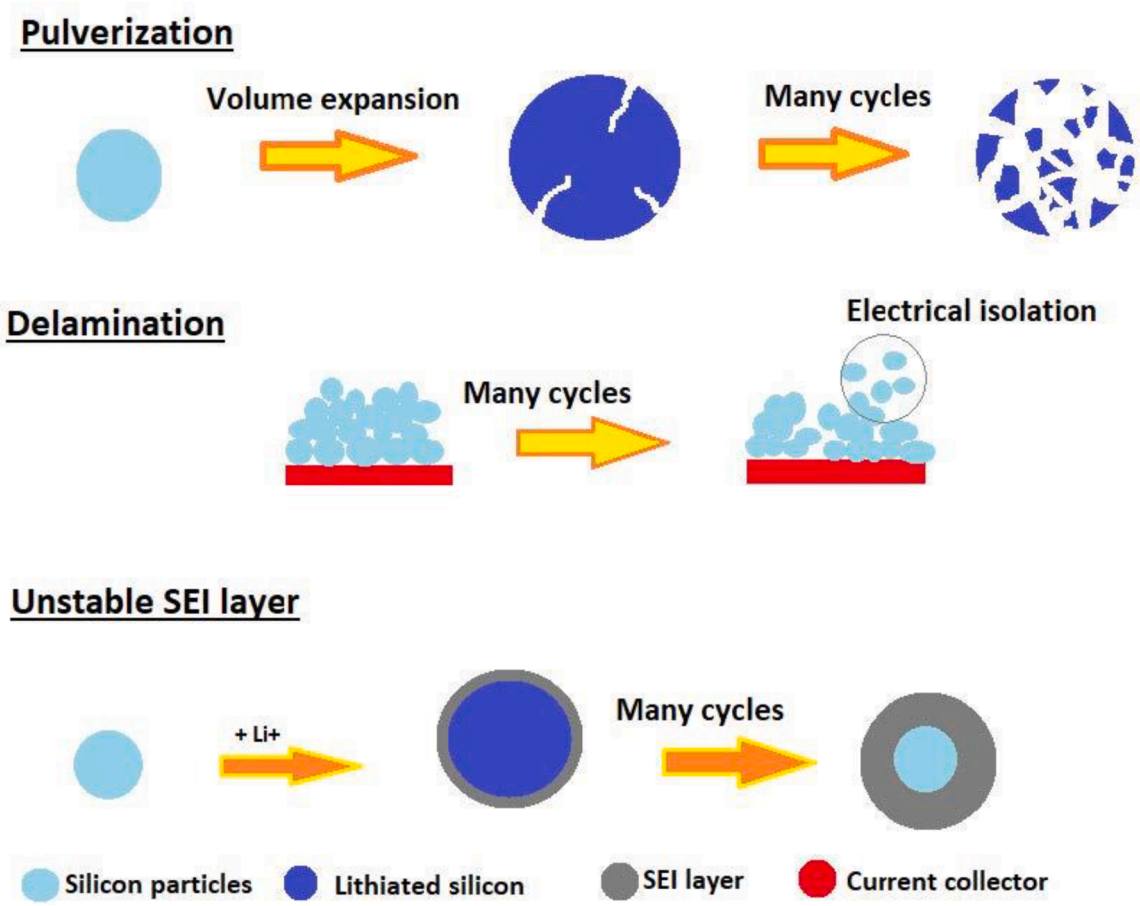

Fig. 10. Diagram showing the challenges of silicon anode materials. Reproduced from Ref [86]. under the terms and conditions of the Creative Commons Attribution 4.0 International License (CC BY 4.0).

voltage hysteresis and iR loss induced by compositional inhomogeneity. However, a sufficient amount of active materials must be implanted to ensure that the overall volumetric energy density is not adversely affected. Another technique worth investigating is introducing another cation or anion into the lattice (similar to the function of a "catalyst") to create a more disordered microstructure and increase ionic and electrical transport characteristics, hence reducing the reaction overpotential. It is postulated that because no more inactive components are introduced, this technique can attain higher energy density than the first. The ternary fluoride $Cu_yFe_{1-y}F_2$solid-solution, for example, has less hysteresis than a pure FeF_2 electrode [83]. One significant problem is preserving the beneficial effect throughout repeated cycling, as Cu is quickly lost by Cu+ dissolution into the liquid electrolyte [83,84].

3.3. Silicon-based compounds

Silicon (Si) has proven to be a very great and exceptional anode material available for lithium-ion battery technology. Among all the known elements, Si possesses the greatest gravimetric and volumetric capacity and is also available at a very affordable cost. It is relatively abundant in the earth crust. It is also not laden with safety risks compared with graphite electrodes, due to its low working potential. Nevertheless, there are huge very significant obstacles limiting the full operation and commercialization of Si anodes. First is the challenge of huge volume variation, which occurs during the lithium-ion insertion/extraction process. The lithiation/de-lithiation process occurs in Si-based electrodes via a conversion reaction. In this process, four lithium atoms are captured byeach silicon atom. The richest phase of the Li-Si being $Li_{22}Si_5$ ($Li_{4.4}Si$) at 415 °C, combined with a high lithium storage capacity of 4200 $mAhg^{-1}$, results in a large volume expansion of approximately 310%. At room temperature, another $Li_{15}Si_4$ phase exists with a lithium capacity of 3579 $mAhg^{-1}$ and a reduced volume expansion capacity of 280% [85]. In the case of anodes made of silicon materials, the high volume fluctuations introduce diverse problems, which include irregular and unsteady electrical contact (delamination), particle cracking, recurrent dynamic creation of SEI layers and ineffective electron transfer as shown in Fig. 10. In reality, therefore, the actual capacity of Si anodes is much lower than what the theoretical values boast, and even its cyclability is quite poor to be deployed for commercial applications. Hence, the development of new-age secondary batteries using Si anodes becomes greatly hindered, especially (among other drawbacks already mentioned) due to its lack of electrical conductivity.

One unique characteristic of silicon is the transition from the crystalline phase to the amorphous phase which it usually undergoes during its first charging and discharging cycle. Silicon in its amorphous state can bear force evenly from all directions, reducing volumetric variation. As a result, avoiding the reverse phase transformation process (back to crystalline silicon) during its subsequent cycles will be highly favorable to the overall operation of LIB electrodes. If the voltage at which lithium intercalation occurs in amorphous silicon is maintained beyond 50 mV, it will be possible to retain silicon in its amorphous state rather than having it transiting back to crystalline Si. In addition to this, the capacity of Si during the first discharge process (4032 $mAhg^{-1}$) also is dramatically reduced when compared to its capacity during the charging process (5149 $mAhg^{-1}$) [87].

Apart from the different drawbacks mentioned which are a result of huge volume fluctuations, another major cause of the huge permanent

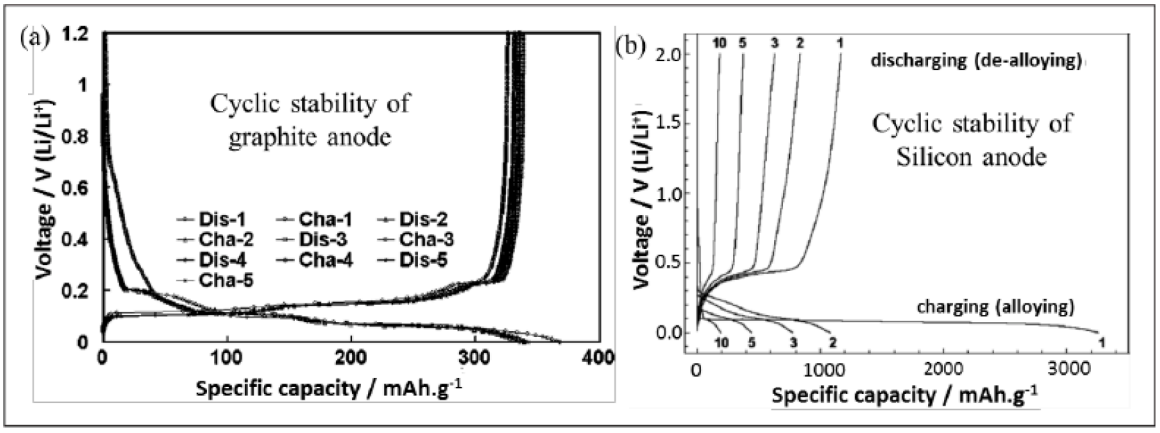

Fig. 11. (a) Galvanostatic discharge/charge profiles during initial electrochemical cycling of (a) graphite [91] and (b) Si (having particle size of ~10 μm) [89] in Li 'half.

loss of capacity may be the solid-state phase transition. The low initial coulombic efficiency (already discussed) is a very major drawback preventing the complete deployment of silicon as a commercial anode material for LIBs.

Another vital issue is that silicon, whether in its crystalline or amorphous form undergoes rapid fade in lithium storage capacity in the first few cycles Fig. 11. shows a comparison of the galvanostatic cyclic stabilities during the first few cycles for graphite and silicon based anodes. Si, for example, exhibits nearly 90% capacity fade after only the first ten cycles [88–90]. Graphitic Carbon-based electrodes, on the other hand, exhibit excellent cyclic stability [91–93]. Moreover, when compared to graphitic carbon, the reversibility of lithiation and delithiation, i.e., coulombic efficiency, is typically low for silicon. This is due to the fact that the fracture/disintegration of silicon during each electrochemical lithiation/delithiation cycle exposes a new surface to the electrolyte, where irreversible surface reactions (including the formation of a solid electrolyte interface (SEI)) continue to occur even after the first cycle [94,95]. Furthermore, the SEI layer originally produced on the surface of silicon appears to be unstable (unlike graphitic carbon for instance) due to the large expansion and contraction in each lithiation and delithiation cycle [94,95]. Such recurrent instances of irreversible surface reactions continue to irreversibly consume lithium from the cell, contributing to a decline in cell capacity in the event of a Li-ion 'full' cell. On a side point, due to the lower Li-diffusivity (DLi) in silicon (Si has DLi of only 10–12 to 10–13 cm^2/s for Si [96,97], as opposed to DLi of 10-7 to 10-9 cm^2/s for graphite [98]), Li-insertion in silicon is a comparatively slower process. In comparison to intercalation (which occurs in graphitic carbon), alloying is a more sophisticated and time-consuming process that involves the 'breakage/distortion' of existing Si-Si bonds in order to generate new Si-Li bonds. As a result, in order to increase the rate capability of Si-based anodes, the 'Li transport distances' in the Si 'host' matrix must be lowered. In other words, in terms of rate capacity, it is preferable to reduce the dimensional scale (particle size, for instance) of silicon. However, the electrode/electrolyte interface area will increase, resulting in the development of detrimental (irreversible) surface reactions [99].

If these significant limitations are allayed, Si anodes will be a major breakthrough in LIB technology.

Taking a leaf from the preceding analysis, researchers have generally accepted the fact that the rational design of the anode's nanostructure is specifically required to overcome the enormous pitfalls of the electrodes made of silicon. According to some studies, Si nanowires perform significantly better than their nanoparticles counterparts because they experience reduced cracking and they possess a specific conductive direction [4]. In addition to this, it was observedthat silicon nanowires transit chiefly to the amorphous phase at 50 mV, while some regions within the core remain crystalline, but at 10 mV, the crystalline regions are completely phased out and the Si nanowires become entirely amorphous [100]. To accommodate silicon's large volume changes, inert matrices are incorporated into anodes of silicon, resulting in the formation of silicon composite electrodes. Inorganic materials are more efficient than polymer matrices at restraining the volume fluctuations of silicon in the process of lithium insertion and extraction. They also offer a consistent and reliable electrical connection with the active material.

Carbon materials serve as better and more functional additives for composite electrodes of silicon. This is owing to their light-weight when compared to other inorganic matrices (TiB_2, TiN, etc.). In the silicon-carbon relationship, each member complements the weakness of the other. While silicon possesses an exceptionally high volumetric and specific capacity but undergoes huge dimensional fluctuations, the carbon matrix can handle volume fluctuations while maintaining structural integrity and electrical stability, however, it lowers battery capacity. From the foregoing, it is worthy to note that the amount of silicon present in the silicon-carbon composite structure is very vital in the rechargeable properties of the battery and it gives rise to two possible development options of silicon-based composite anodes. The first option is the composite anode with poor capacity and excellent cyclability, while the second option is the composite anode with excellent capacity and low cyclability. However, it is common knowledge that increasing the silicon content in silicon-carbon composite to a maximum to achieve a high capacity performance leads to numerous adverse consequences, among which are incompatible battery system, poor processability, and low economic efficiency. Ren et al [101]. discovered that when the C/Si ratio is 1:0.2, the composite anodes exhibit the greatest initial coulombic efficiency compared to 1:0.1 and 1:0.3 ratios. This is because a mild increase in the silicon content can lead to a significant rise in the porosity of the silicon/carbon microspheres, whereas as the C/Si ratio decreases, some silicon particles agglomerate.

Presently, self-designed assembly systems are the central focus of research studies on high capacity silicon anodes. In summary, both present and future researchon Si/C electrode materials are primarily centered on improving cyclability, elevated charge and discharge rate, increased energy density, stable properties, low safety risks and large-scale production at minimalcosts [102–104].

There are a couple of major established methods for the synthesis of silicon/carbon composite anode materials. These methods include electrospinning, pyrolysis, hydrothermal, mechanical milling, CVD, and sol-gel methods. It is, however, painful to note that majority of the conventional methods of synthesis have poor results and are not environmentally friendly, consequently the invention of extensible and adaptable processes leading to the achievement of high efficiency and maximum yield is necessary to ensure the possible and commercial

deployment of silicon composite anodes. Ren et al [101]. described a cost-friendly and environmentally safe method for producing porous silicon/carbon microspheres (GPSCMs). They used sucrose to bind silicon nanoparticles to porous carbon microspheres and graphitized needle coke produced from industrial waste materials served as a carbon source.

In the design of silicon composite structures, the concept of utmost priority is to address the basic drawbacks of the silicon anode by providing additional vacancies to accommodate its expansion. This is achieved by employing carbon as a conductive matrix. Hertzberg et al [105]. developed a Si@C composite (termed Si-in-C tubes) which basically comprises a silicon nanotube within a carbon nanotube. During lithiation, the expansion of silicon nanotube is directed inward as a result of the constraints of the carbon nanotube (CNT) 'shell' and during delithiation, it also contracts easily within the CNT. The tiny openings on the walls (pores) of CNTs allow for enough variation in the dimensions of silicon during expansion and contraction in order to guarantee complete structural coherence. The Si-in-C composite as an anode exhibited improved electrochemical performance in a battery performance test. They also carried out tests on the frameworks of several silicon structures with different wall thickness levels and discovered a delamination activity for the 33 and 46 wt% silicon samples. The delamination of silicon nanotubes from carbon nanotubes brought about a decrease in the electrical contact. The 9 and 46 wt% samples of silicon exhibited the greatest capacity quite close to theoretical capacity. However, even though the coulombic efficiency was up to 99.5% beyond the first and subsequent cycles, the coulombic efficiency in the initial cycle was just about 75%.

Aside from techniques that increase the wall thicknesses of silicon and carbon, which have been developed, more effective modification methods are necessary. Wu et al [106]. suggested a SiNPs@CNTs model with silicon nanoparticles dispersed on the wall openings (pores) of carbon nanotubes. The expansion/contraction of silicon nanoparticles and the stability of the solid electrolyte interface layer can be regulated independently by enabling the unimpeded expansion of silicon NPs by making use of free spaces between the particles while preventing the silicon NPs from making contact with the electrolyte with the aid of carbon nanotubes. Ji et al [107]. created yet another innovative self-supported anode. Using aqueous suspensions, they created Silicon-Graphene-Ultrathin Graphite Foam (Si-Graphene-UGF) composite where Silicon nanoparticles encased within a graphene cover a UGF surface. Beside the assets and benefits of graphene, the UGF surface not only ensures optimal electronic contact in the electrode but also eliminates the need for bulky silicon loading. Liu et al [108]. created a Si@C composite having the shape of a pomegranate. Here, each silicon particle is enclosed within a carbon sphere which provides a fully restricted open space for expansion and contraction of silicon in the process of Li lithiation/de-lithiation. By design, the carbon shell will be occupied fully in the lithiation process. For 9% carbon, the Initial Coulombic Efficiencies (ICE) may be up to 82%, and subsequent Coulombic Efficiencies (up to 1000 cycles), on average, may be up to 99.87%. The relatively low ICE may be attributed to the amorphous morphology of the carbon shell; hence the search for better alternatives for carbon shell may lead to a greater improvement of the ICE so as to exceed 85%. One great advantage of the silicon pomegranate anode is that its manufacturing procedure is devoid of complicated processes and it is well suited and adaptable to the current battery system.

3.3.1. *Electrolyte selection for Si-based anodes*

Electrolytes serve the purpose of providing an effective path for the transfer of lithium ions while at the same time remaining electronically non-conductive. An elevated dielectric constant and reduced electrolyte viscosity at common operating temperatures are prerequisite for obtaining an increased ion conduction capacity [109]. Further to that, because Si is the anode, traditional electrolytes containing dimethyl carbonate (DMC) or diethyl carbonate (DEC) and ethylene carbonate (EC), among others, will invariably be reduced within the potential range of silicon [110]. The only component left for scientists and engineers to modify is the formation of a one-time, stable SEI that protects the Si surface against further SEI growth. As have been elaborated in previous discussions, this poses an obvious limitation for silicon due to frequent volume variations, pulverization, and the resulting creation of new surface area, thus paving way for new SEI formation [111]. Furthermore, the continuous expansion and contraction of silicon result in an unfavorable separation of SEI from the surface of the active material, revealing new surface area for more SEI generation. Consequently, researchers on electrolytes have looked for solutions to these problems in electrolyte salts, solvents, and electrolyte additives.

Electrolyte salts and solvents are somewhat more established among these alternative solutions, owing to extensive research on electrolytes for normal LIBs. Electrolyte additives, which can be chosen or adjusted to address Si-related difficulties, are a promising avenue for increasing Si anode performance. Electrolyte additives such as succinic anhydride [112], lithium bis(oxalate)borate (LiBOB) [113], lithium difluro(oxalato)borate (LiDFOB) [114], vinylene carbonate (VC) [115], and fluoroethylene carbonate (FEC) [116] have been shown to extend cycle life and CE. Dalavi et al. published an intriguing paper that did a direct comparison of most of the above electrolyte additions [114]. Despite the lack of mechanistic description in this paper, it gave a good overview of what to expect from each additive under the same experimental settings. It is clear that switching the solvent from EC to propylene carbonate (PC) has a negative impact on the cell performance in terms of cycle life. Furthermore, because the cycle life deterioration is most likely owing to strong SEI development and reformation, PC has an extremely low CE. This means that the PC electrolyte is continually degraded throughout each cycle, with negligible passivation (protective) action. This effect is exacerbated by the pulverization of silicon during cycling, which creates even more surface area for PC to degrade on. PC-based electrolytes have also been shown to be ineffective in preserving the stability of the SEI, and are known to intercalate into the layers of graphite, resulting in graphite layer exfoliation [117]. When the other additions were evaluated, Dalavi's findings indicated that FEC and VC are the most effective electrolyte additives. Both of these additives were able to keep their capacity retention and CE levels high.

During cycling, EC and DEC disintegrate, depositing polymeric and oligomeric molecules on the surface of silicon. When $LiPF_6$ degrades on the anode active material's surface, whether graphite or Si, LiF is produced in SEI. There have been disagreements concerning the function of LiF in SEI, and a full survey to better understand it has yet to be completed [118]. At around 1 V against Li/Li, VC decomposes ahead of the degradation of EC and DEC, generating an SEI layer on the surface of Si that is impervious to the electrolyte [119]. Unmodified EC and DEC electrolyte forms an SEI layer that is somewhat electrolyte susceptible. It's vital to note that one of an SEI's most significant qualities is its ability to transport Li ions while remaining impermeable to electrolyte. Electrolyte molecules are physically detached from Si and effectively prevented from further breakdown on the Si surface when a VC-derived first SEI layer is formed.

Many peer-reviewed papers mention FEC as one of the most common electrolyte additives. It offers various advantages in addition to its steady cycle performance, such as a low melting point and low flammability [120]. Because FEC creates VC, it is reasonable to assume that it will also protect Si [116]. Xu et al. investigated the mechanism through which FEC benefits from its use as an additive [121]. Xu compared an FEC-added electrolyte system to an additive-free silicon LIB, as in earlier works. The outcome is similar with prior results, demonstrating a significant increase in capacity retention and CE. Furthermore, compared to the broad SEI layer enveloping the Si particle in the unmodified cells, Si particles in the FEC modified cells seemed to have a substantially more compact SEI layer. The FEC modified cells would have a decreased mass transfer resistance as a result of this. This disparity, according to Xu, is due to the fact that FEC decomposes at a voltage of 1.3 V against

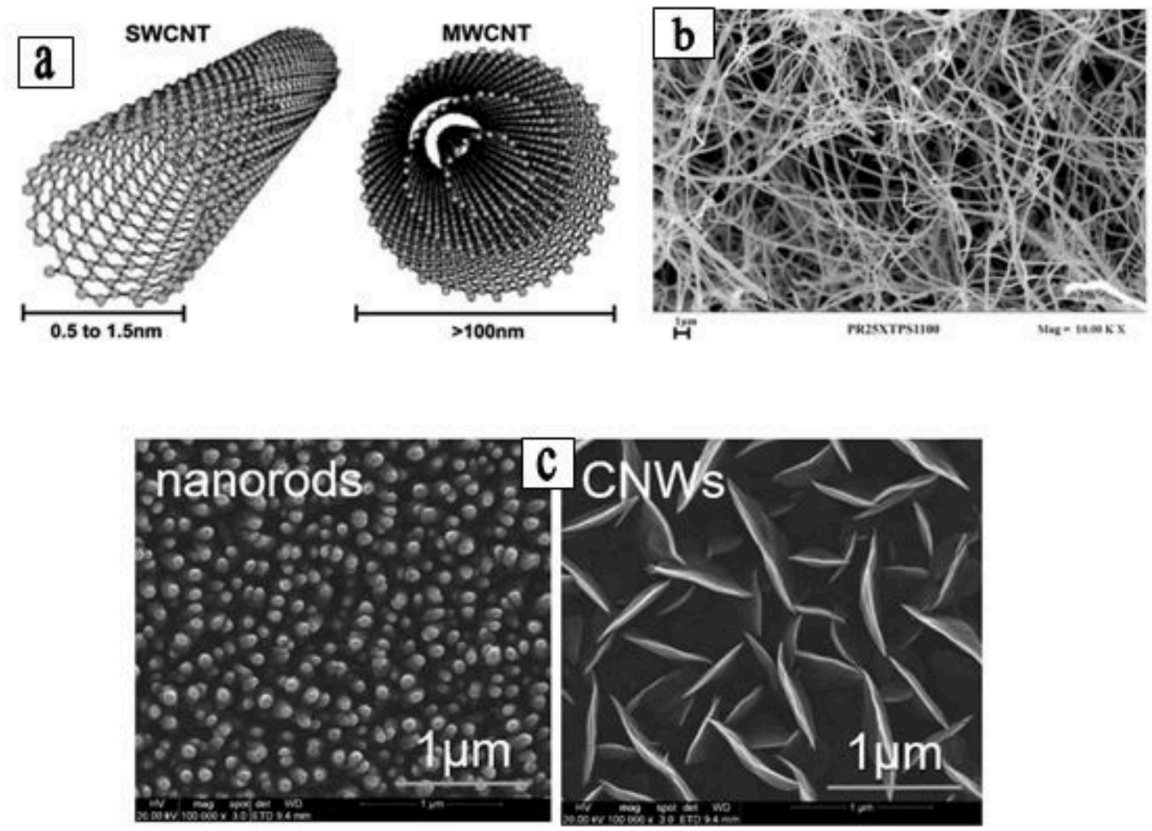

Fig. 12. . (a) Schematic diagram showing the single-walled carbon nanotube (SWCNT) and multi-walled carbon nanotube (MWCNT) (Reproduced from Ref [126]. under the terms and conditions of the Creative Commons Attribution 3.0 Unported (CC BY 3.0) licence; (b) SEM image of carbon nanofibers (CNFs)(Reproduced from Ref [125]. under the terms and conditions of the Creative Commons license, CC–BY 4.0); (c) SEM images of carbon nanorods (CNRs) and carbon nanowires (CNWs), (Reproduced from Ref [127]. under the terms and conditions of the Creative Commons Attribution 4.0 International License).

Li/Li^+, which is substantially greater than EC and DEC. The carbon signal of the SEI layer shows a modest decline in XPS data of the fresh electrode and electrodes discharged to 0.9 V (before the initiation of EC and DEC breakdown). This peak is often ascribed to the carbonate species because of a shift in the C 1s peak from 290 to 290.8 eV, although this shift is most likely owing to the creation of a type of fluorocarbonate, a result presumably from FEC's ring opening [122]. This shows that FEC decomposes first during discharge, allowing for the formation of a protective layer on the Si surface before the EC/DEC decomposition [120].

Another advantage of FEC may be its capacity to produce more fluorinated phosphoric oxides. These novel species may interact with $LiPF_6$'s intermediate breakdown products, stabilizing them and preventing further decomposition. To conclude, Xu argued that not only the thickness of the SEI, but also the chemical composition and structural features of the material are critical parameters. This is crucial from a conceptual standpoint, because when FEC decomposes on Si, it essentially generates a Si/polymer composite. As a result, FEC may offer advantages not only in terms of chemistry, but also in terms of structural integrity, comparable to other Si/C composites. As a result, the mechanical characteristics of the SEI, such as stiffness and elasticity, might be tweaked to give new directions for silicon LIB anode electrolyte research in the future.

3.3.2. *Future perspective for silicon-based anodes*

With the rising demand for batteries with high energy density, LIBs anodes made from silicon-based materials have become a highly priotized study focus and have witnessed significant progress. Presently, the application of silicon anodes in electrochemical energy storage is grossly limited by two major bottlenecks: large volume variations and low electrical conductivity. As a result, the silicon-based material's future development will focus on both increased capacity, improved cycle stability as well as SEI stability.

3.4. *Carbon based compounds*

Carbon is now used primarily in commercial lithium-ion battery anodes due to its advantageous properties such as widespread availability, outstanding electronic conductivity, low cost and a favorable hierarchical arrangement for Li-ion insertion. However, certain drawbacks of graphite anodes, which include decreased rate capacity, low specific capacity, as well as safety risks, have prompted further research into the performance optimization ofof carbon-based material anodes. Dendrites are formed as a result of the slow working potential of carbon and the sustained deposition of lithium ions. These architectures are the source of the safety concerns, which are significant limitations that carbon-based anodes have that prevent their widespread commercialization.

There are two types of carbonaceous materials: graphitic carbon (GC) and non-graphitic carbon (NGC). Graphitic carbon is highly crystalline, whereas non-graphitic carbon is amorphous. The former and latter are commonly referred to as 'soft' and 'hard' carbon, respectively. This is because NGC possesses a significantly higher mechanical hardness. Carbon atoms exist in graphite structures as sp [2] or sp [3] hybridization, and the entire carbon material structure is made up of graphene planes piled up over each other. Graphenes are made up of carbon double bonds. No more than six carbon atoms cling to one lithium-ion forming LiC_6. LiC_6 occurs most frequently in carbon anodes, resulting in a theoretical capacity of 372 $mAhg^{-1}$, whereas amorphous carbon structures take in fewer amounts of lithium. The carbon material

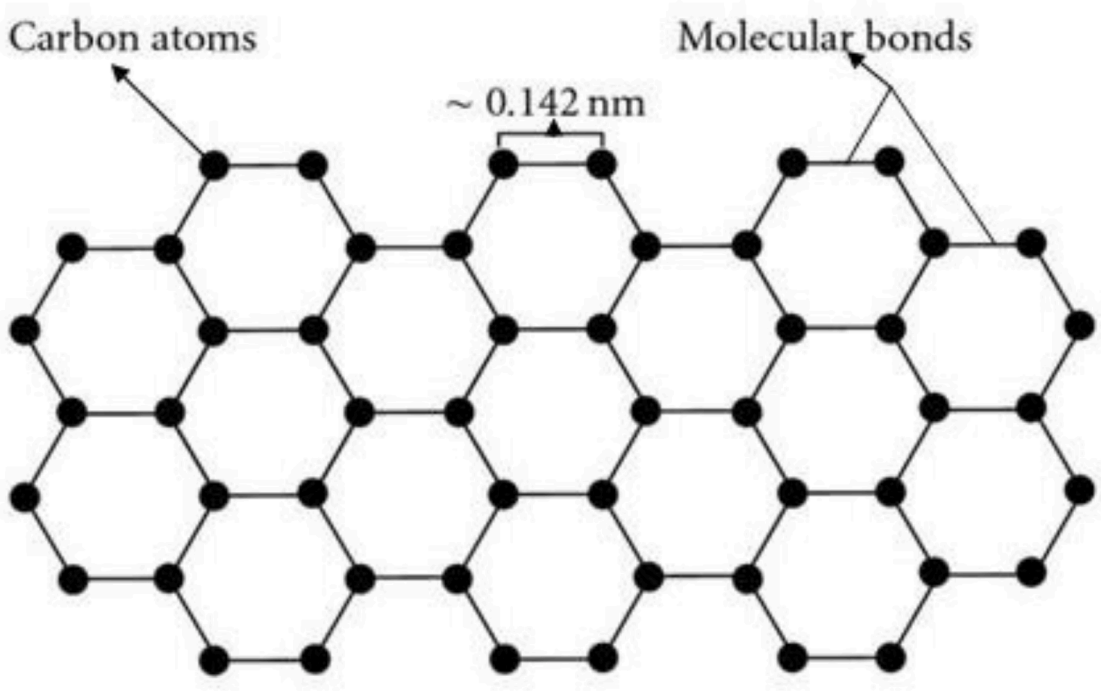

Fig. 13. Schematic diagram showing the structure of a graphene sheet. (Modified from Ref [129]. under the terms and conditions of Creative Commons Attribution License).

anode's lithium insertion/extraction process is stated thus:

$$Li^{+} + e + nC = LiC_n \quad (1)$$

In Eq. (1), n has values of 6–12. Carbon's microstructure, crystallinity, and morphology all have a significant effect on the nature, attributes and capacity of the lithiation compound. Different carbon materials possess varying bond-distances, with varying stacked-layer thicknesses, resulting in diverse lithiation capacities. Presently, in the electric industry, it is observed and recorded that coke or hard carbon, as an anode, possesses excellent stability of cycles, whereas graphite electrodes exhibit high energy density and excellent capacity. The proceeding sections cover the intercalation capacities of diverse carbon nano-structures in 1-dimension, 2-dimensions, and 3-dimensions, as well as the methods of the anode synthesis.

3.4.1. 1-Dimensional carbon nanostructures (nanotubes, nanorods and nanofibers (CNTs))

CNTs are graphenes rolled into sheets having one or more layers. They can be single-walled, referred to as SWCNTs (single-wall carbon nanotubes) or multi-walled, referred to as MWCNTs (multi-wall carbon nanotubes) as shown in Fig. 12a. CNT anodes are more capable of storing and converting energy than standard graphite electrodes. This is due to their impressive conductivity and structural stability. It has been observed that for the direction or the path of transfer of charges, lithium ions undergo diffusion along the axial direction, as opposed to the radial direction [123]. According to research, the purity of carbon nanotube electrodes and the type of additives influence the reversible capacity by regulating the creation of a Solid Electrolyte Interface [124]. In the anode, carbon nanotubes (CNTs) can take the shape of an entangled random system (ECNT) or an array architecture (CNTA). Furthermore, CNTs can serve as the conductive substrate, the binder and the active material all at the same time to form a so-called free-standing electrode. Although the interior and posterior walls of CNTs can both adsorb lithium ions, the adsorption capacity of the internal walls is higher [125].

Surprisingly, simple changes in some synthesis techniques will lead to the formation of CNWs (carbon nanowalls) or carbon nanorods rather than Carbon Nanotubes. The morphology of the carbon layer under certain techniques depends largely on the pressure and gas flow rate as shown by Fig 12c. When the gas flow rate is high and the pressure low, nanorods are formed, while at average pressure and gas flow rate, CNWs are formed [126]. Carbon configuration varies significantly among the above-mentioned carbon nanostructures, while CNTs are made up of well-arranged graphitic carbon having sp [2] bonds, CNWs are made up of amorphous carbon with sp [2] and sp [3] mixed hybridization. For carbon nanofibers, they are nanostructures of graphene with cylindrical-shaped layers (Fig 12b). When they are wrapped into perfect cylinders, they become carbon nanotubes [125].

3.4.2. Graphene: (2-Dimensional carbon nanostructure)

Graphenes are simply single graphite sheets. They are one-atom-thick lattices of carbon atoms systematically arranged in hexagonal rings as shown in Fig. 13. They possess large surface areas and are highly conductive. The theoretical specific capacity of graphene (744 $mAhg^{-1}$) is more than twice the capacity of graphite (372 $mAhg^{-1}$) with a smaller surface area because the two faces of the sheets are both accessible to ions and electrons in the electrolyte. Furthermore, the mechanical flexibility of graphene is extremely beneficial to portable and flexible electronic devices. Despite these outstanding features, graphene does have some drawbacks; the volumetric capacity of graphene sheets is quite reduced as a result of their low density. The extraordinary qualities of graphene sheets may be lost if they are re-stacked. In addition, the synthesis of huge surface area and highly conductive graphene is complex, and controlling the development of impurities/defects on graphene sheets is exceedingly tough [4].

The techniques for graphene synthesis are classified as "top-down" or "bottom-up" [128]. Graphene oxide reduction, mechanical exfoliation, SiC-based synthesis, and liquid phase exfoliation are examples of "top-down" techniques, which typically give low yields. Similarly, chemical vapor deposition (CVD) and surface segregation processes are common examples of "bottom-up" techniques. In addition to high yield, graphene films produced using surface segregation and CVD techniques have outstanding scalability and large surface area [4].

Graphene materials have recently emerged as one of the most

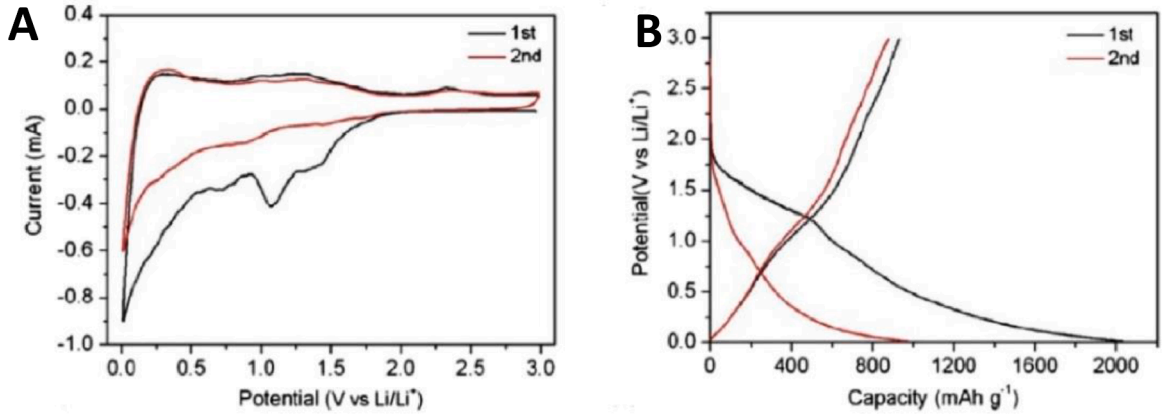

Fig. 14. Diagram showing (a) CV profile and (b) charge/discharge curves of PG for the first and second cycles at a current density of 50 mA/g. Reproduced from Ref [142].

promising alternatives for LIB anodes because to its high theoretical specific capacity (744 mAh/g), huge specific surface area, superior electrical conductivity, efficient carrier mobility, and broad electrochemical window. However, due to the high aspect ratio of graphene nanosheets, the Li-ion transport paths are lengthy. Furthermore, because to the intense π-π stacking and van der Waals interaction between layers, graphene has a high natural inclination to aggregate. These flaws not only reduce the electrode's high specific surface area and active sites for Li-ion storage, but also its rate performance [130–132]. The aforementioned difficulties can be solved via heteroatom doping of graphene sheets (with sulfur, nitrogen, and boron) otherwise known as fuctionalized graphene which include S-doped, N-doped, B-doped, Halogen-doped and co-doped functionalized graphene anode materials, among which N-doped graphene has been extensively researched [133]. It has been revealed that several forms of functionalized graphene materials may be generated in a one-step electrochemical exfoliation of graphite by adjusting the electrolyte [133]. In general, previous research has demonstrated that N-doped graphene may be produced by electrochemical exfoliation of graphite by varying the electrolyte or electrodes [134–136]. However, there have been few research on the electrochemical performance of doped-graphene as anode for LIBs generated by electrochemical exfoliation of graphite [133]. Nitric acid (HNO_3) can be used as an efficient electrolyte for simultaneous graphite exfoliation and N doping of the graphene lattice. For example, Lokhande et al [137]. developed N-doped graphene as an anode for LIBs via electrochemical exfoliation of graphite. They used cyclic voltammetry with varied potential ranges in 5.0 M HNO_3 electrolyte. The findings of the Raman study revealed that increasing the anodically voltages enhanced the defect density of the samples. Their findings demonstrated that the applied voltage has a considerable impact on the electrochemical performance of the synthesized N-doped graphene.

Another way to arrest the challenges above is by fabricating various types of two-dimensional (2D) holey graphene and three-dimensional (3D) porous graphene (discussed in next section). In general, 2D holey graphene materials may be created by depositing in-plane carbon vacancy defects onto graphene nanosheets [133]. Holes facilitate Li-ion diffusion through the layers during lithiation/de-lithiation processes, enhancing the rate capability of LIBs even in the presence of restacking.

It is clear that the preparation technique has a significant impact on the microstructure of porous graphene materials, such as pore

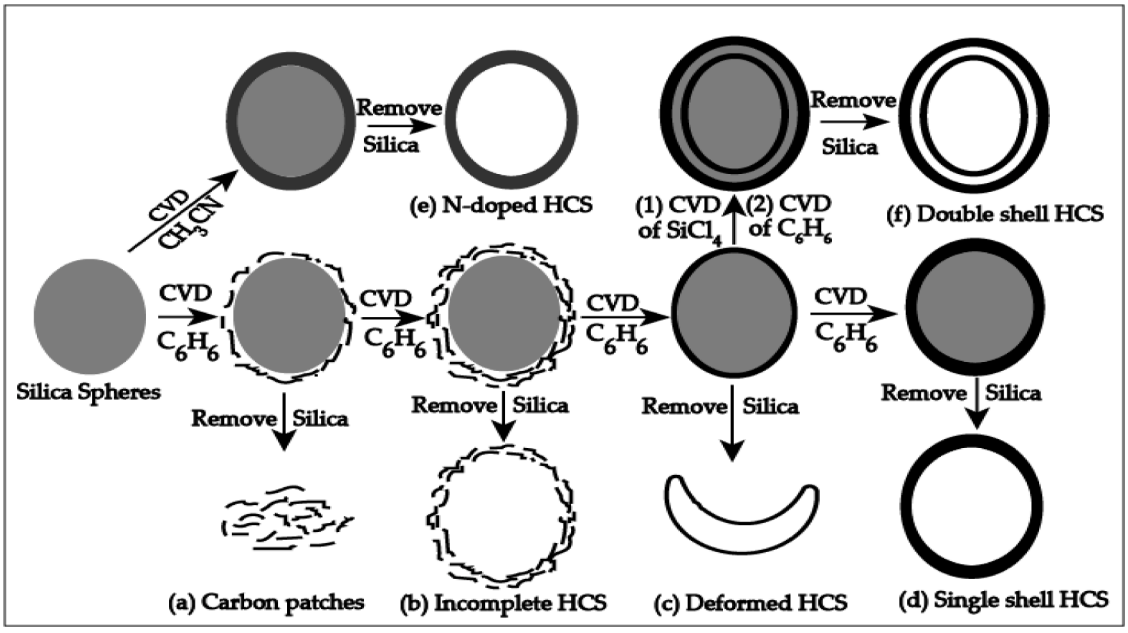

Fig. 15. Schematic diagram showing the steps for the production of different carbon spheres (HCSs) (Modified from Ref [4]. under the terms and conditions of the creative commons attribution 3.0 unported (CC BY 3.0) licence).

morphologies and distributions, which affect performance. The production techniques of holey graphene are classified in many ways in the literature [138–140]. Cao et al [141]. categorized the production techniques of holey graphene with the potential for large-scale production into three categories: (1) thermal etching, (2) wet-chemical etching, and (3) catalytic etching, all of which are template-free processes. Furthermore, template-assisted techniques may be used to create holey graphene. For instance, Roberts et al [142]. employed simple metal etching as an effective technique for large-scale porous graphene (PG) production. The results revealed that extending the reaction time resulted in the creation of bigger holes with irregular shapes. Furthermore, when the grapheme oxide (GO)/nickel (Ni) ratio increased, the density of pores dropped. In the meanwhile, additional metals (Fe, Cu, and Co) were utilized as etchants to make PG. The results showed that the type of metallic etchant used had an effect on the density and size of the pores.

The electrochemical performance of the PG anode indicated that the early irreversible consumption of Li-ions and the inevitable creation of an SEI layer on the surface of the electrode resulted in substantial losses of specific capacity in the first cycle, as illustrated in Fig. 14a and b. The capacity observed above and below 0.5 V was caused by lithium ion insertion/extraction from faults such as pores. The absence of a potential plateau was caused by disordered stacking of graphene layers. The first charge specific capacity of the PG electrode was 933 mAh/g at 50 mA/g, which was significantly higher than the RGO electrode (548 mAh/g in the first cycle).

3.4.3. 3-Dimensional porous carbon structure (core-shell and carbon sphere structure)

Diverse research on the improvement of the morphology and quality of the porous carbon structure has led to the development of several effective CSs (carbon spheres) manufacturing procedures as shown in Fig. 15. The properties of CSs differ depending on the method of synthesis employed. CVD is the most common method of producing CS. The carbon precursor in the gaseous state first decomposes, deposits, and then undergoes heating, all at high temperatures, to form spheres [143]. A huge variety of carbon-containing materials can serve as CS precursors. The size of the obtained carbon sphere can also be manipulated (50–1000 nm) by adjusting process variables such as reaction time, reaction temperature, and feed time. According to reports, the processed carbon spheres have simultaneous sp [2] and sp [3] bonding and exhibit chemical and structural stability up to 900 °C in sterile and unreactive atmospheric conditions or a little less than 600 °C in open air [144].

3.4.4. Future perspective for carbon-based anodes

Regardless the fact that studies and research on LIB anodes made from carbon based materials have gained a high altitude and almost attained perfection, there is still room for the creation of high magnification and increased current research on graphite materials. On economic (price) and safety basis, future studies will focus on the dynamic behavior of carbon anode materials.

4. Conclusion

As a result of their highly attractive properties such as elevated power density and great capacity, LIBs will have an ever-increasing effect and impact on our lives in the coming years. LIBs technology provides an entirely new and distinct approach to energy storage and applications. Hence they have stood out as an indispensable alternative for both present and future energy operations, storage and adaptations. Appliances and devices which feature in the daily activities of man which make life easier (from smartphones, digital cameras, and laptops to Electric Vehicles and Hybrid Electric Vehicles) all place much demands on LIBs for maximum energy storage while minimizing density. Research studies in the field of lithium-ion batteries within the past few decades have been quite exciting and, without doubt, as new novel materials and strategies are being developed. In recent years, the need to develop anode materials that will serve as possible commercial alternatives for the conventional graphite anodes, whose capacities have failed to meet up with the requirements for future high-performance lithium-ion batteries, have come to the fore. Several studies and innovations have also addressed this pressing need. This has resulted in the modeling and development of several novel anode materials that may compete favorably with graphite anodes. Some of these anode materials were studied under four basic categories, namely:Alloy Materials, Conversion-type Transition Metal compounds, Silicon-based compounds, and Carbon-based compounds. Each of the categories had promising features and capacities but was also laden with drawbacks limiting their full performance. Diverse modelshave been developed to mitigate the deficiencies of the anode materials. For example, silicon anode as well as other anode materials materials experience very large volume changes during the lithiation/de-lithiation process, giving rise to an unstable SEI layer, loss of electrical contact between the active material and the current collector, an eventual pulverization of the material and huge capacity loss. In addition, some of these materials experience poor conductivity giving rise to low capacity. To address these challenges, researchers incorporated inert matrices, such as carbon, into anodes of silicon, resulting in the formation of silicon composite electrodes. The carbon matrix was able to handle silicon's volume fluctuations while maintaining structural integrity and electrical stability. Consequently, the Si/C composite as an anode exhibited improved electrochemical performance in a battery performance test. This review offers a holistic view of recent innovations and advancements in anode materials for Lithium-ion batteries and provide a broad sight on the prospects the field of LIBs holds for energy conversion, storage and applications (Table 1).

Table 1
The benefits and drawbacks of different anode materials for lithium-ion batteries.

Anode	Benefits	Limitations
Alloys	(a.) Specific capacity is high (400–2300 $mAhg^{-1}$)	(a.) Electronic conductivity is low
	(b.) Offers good security (i.e. no safety risks involved)	(b.) Huge change in volume (100%)
Carbon	(a.) Electronic conductivity is high	(a.) It has a low specific capacity
	(b.) Commendable hierarchical structure	(b.) It has a low rate capacity
	(c.) Inexpensive resources which are also abundant	(c.) It is associated with safety risks
Transition metal oxides	(a.) Specific capacity is commendably high (600–1000 $mAhg^{-1}$)	(a.) Coulombic efficiency is poor
	(b.) Its shape and size are highly stable at charge/discharge cycle	(b.) Potential hysteresis is large
Silicon	(a.) It has a very high specific capacity (3579 mAh^{-1})	(a.) Very large change in volume (300%)
	(b.) Resources are abundant, clean and inexpensive	

Declaration of Competing Interest

The authors declare that they have no known competing financial interests or personal relationships that could have appeared to influence the work reported in this paper.

Acknowledgments

We are grateful to the Royal Society and the African Academy of Sciences for the Award of a FLAIR Fellowship to Dr A. C. Nwanya (Grant No.: FLR\RI\201225). We also appreciate and acknowledge the African Centre of Excellence for Sustainable Power and Energy Development, ACE-SPED, University of Nigeria, Nsukka for their support.

References

[1] P. Roy, S.K. Srivastava, Nanostructured anode materials for lithium ion batteries, J. Mater. Chem. A 3 (2015) 2454–2484.

[2] M. Osiak, H. Geaney, E. Armstrong, C. O'Dwyer, Structuring materials for lithium-ion batteries: advancements in nanomaterial structure, composition, and defined assembly on cell performance, J. Mater. Chem. A 2 (2014) 9433.

[3] A. Hammouche, E. Karden, R.W. De Doncker, Monitoring state-of-charge of Ni–MH and Ni–Cd batteries using impedance spectroscopy, J. Power Sources 127 (2004) 105–111.

[4] W. Qi, J.G. Shapter, Q. Wu, T. Yin, G. Gao, D. Cui, Nanostructured anode materials for lithium-ion batteries: principle, recent progress and future perspectives, J. Mater. Chem. A 5 (2017) 19521–19540.

[5] Y. Kim, W. Song, S.Y. Lee, C. Jeon, W. Jung, M. Kim, C.Y. Park, Low-temperature synthesis of graphene on nickel foil by microwave plasma chemical vapor deposition, Appl. Phys. Lett. 98 (2011) 263106–2631063.

[6] J. Speirs, M. Contestabile, Y. Houari, R. Gross, The future of lithium availability for electric vehicle batteries, Renew. Sustain. Energy Rev. 35 (2014) 183–193.

[7] L. Su, Y. Jing, Z. Zhou, Li ion battery materials with core–shell nanostructures, Nanoscale 3 (2011) 3967–3983.

[8] B. Gao, S. Sinha, L. Fleming, O. Zhou, Alloy formation in nanostructured silicon, Adv. Mater. 13 (2001) 816.

[9] M. Wachtler, M. Winter, J.O. Besenhard, Anodic materials for rechargeable Li-batteries, J. Power Sources 105 (2002) 151.

[10] J.W. Kim, J.H. Ryu, K.T. Lee, S.M. Oh, Improvement of silicon powder negative electrodes by copper electroless deposition for lithium secondary batteries, J. Power Sources 147 (2005) 227.

[11] J.T. Vaughey, L. Fransson, H.A. Swinger, K. Edstrom, M.M. Thackeray, Alternative anode materials for lithium-ion batteries: a study of Ag_3Sb, J. Power Sources 119–121 (2003) 64.

[12] L.Y. Beaulieu, K.W. Eberman, R.L. Turner, L.J. Krause, J.R. Dahn, Colossal reversible volume changes in lithium alloys, Electrochem. Solid State Lett. 4 (2001) A137.

[13] Y. Zhong, M. Yang, X. Zhou, Z. Zhou, Structural design for anodes of lithium-ion batteries: emerging horizons from materials to electrodes, Mater. Horiz. 2 (2015) 553–566.

[14] C.M. Park, S. Yoon, S.I. Lee, J.H. Kim, J.H. Jung, H.J. Sohn, High-rate capability and enhanced cyclability of antimony-based composites for lithium rechargeable batteries, J. Electrochem. Soc. 154 (2007) A917.

[15] Y. Wang, F. Su, C.D. Wood, J.Y. Lee, X.S. Zhao, Preparation and characterization of carbon nanospheres as anode materials in lithium-ion secondary batteries, Ind. Eng. Chem. Res. 47 (2008) 2294–2300.

[16] W.M. Zhang, J.S. Hu, Y.G. Guo, S.F. Zheng, L.S. Zhong, W.G. Song, L.J. Wan, Tin-nanoparticles encapsulated in elastic hollow carbon spheres for high-performance anode material in lithium-ion batteries, Adv. Mater. 20 (2008) 1160–1165.

[17] W. Qi, J.G. Shapter, Q. Wu, T. Yin, G. Gao, D. Cui, Nanostructured anode materials for lithium-ion batteries: principle, recent progress and future perspectives, J. Mater. Chem. A 5 (2017) 19521–19540.

[18] M.A. Reddy, U.V. Varadaraju, NbSb2 as an anode material for Li-ion batteries, J. Power Sources 159 (2006) 336–339.

[19] J. Yin, M. Wada, S. Yoshida, K. Ishihara, S. TanaseandT. Sakai, New Ag-Sn alloy anode materials for lithium-ion batteries, J. Electrochem. Soc. A 150 (2003) 1129.

[20] O. Mao, J.R. Dahn, Mechanically alloyed Sn-Fe(-C) powders as anode materials for Li-Ion batteries: III. Sn_2Fe : $SnFe_3$ C active/inactive composites, J. Electrochem. Soc. 146 (1999) 423–427.

[21] Y. Lu, L. Yu, X.W. Lou, Nanostructured conversion-type anode materials for advanced lithium-ion batteries, Chem 4 (5) (2018) 972–996.

[22] X. Wang, J. Wang, Z. Chen, K. Yang, Z. Zhang, Z. Shi, et al., Yolk-double shell Fe_3O_4@C@C composite as high-performance anode materials for lithium-ion batteries, J. Alloy. Compd. 822 (2020), 153656.

[23] S.H. Oh, O.H. Kwon, Y.C. Kang, J. Kim, J.S. Cho, Highly integrated and interconnected CNT hybrid nanofibers decorated with α-iron oxide as freestanding anodes for flexible lithium polymer batteries, J. Mater. Chem. A 7 (2019) 12480–12488.

[24] A.O. Soge, Anode materials for lithium-based batteries: a review, JMSRR 5 (3) (2020) 21–39.

[25] T.D. Hatchard, J.R. Dahn, *In situ* XRD and electrochemical study of the reaction of lithium with amorphous silicon, J. Electrochem. Soc. 151 (2004) 838–842.

[26] H. Wu, G. Chan, J.W. Choi, I. Ryu, Y. Yao, M.T. McDowell, et al., Stable cycling of double-walled silicon nanotube battery anodes through solid–electrolyte interphase control, Nat. Nanotechnol. 7 (2012) 310–315.

[27] Y. Yao, M.T. McDowell, I. Ryu, H. Wu, N.A. Liu, L.B. Hu, et al., Interconnected silicon hollow nanospheres for lithium-ion battery anodes with long cycle life, Nano Lett. 11 (2011) 2949–2954.

[28] B.Y. Guan, Y. Lu, Y. Wang, M. Wu, X.W. Lou, Porous iron–cobalt alloy/nitrogen-doped carbon cages synthesized via pyrolysis of complex metal–organic framework hybrids for oxygen reduction, Adv. Funct. Mater. 28 (10) (2018) 1706738–1706751.

[29] J. Dai, J. Li, Q. Zhang, M. Liao, T. Duan, W. Yao, Microstructures fabricated from MOF template as advanced lithium-ion battery anode, Mater. Lett. 236 (2018) 483–486.

[30] D. Chen, G. Ji, B. Ding, Y. Ma, B. Qu, W. Chen, J.Y. Lee, Double transition-metal chalcogenide as a high-performance lithium-ion battery anode material, Ind. Eng. Chem. Res. 53 (46) (2014) 17901–17908.

[31] M. Sajjad, F. Cheng, W. Lu, Research progress in transition metal chalcogenide based anodes for K-ion hybrid capacitor applications: a mini-review, RSC Adv. 11 (2021) 25450–25460.

[32] Z. Qi, Y. Wu, X. Li, Y. Qu, Y. Yang, D. Mei, Microwave-assisted synthesis of $CuC_2O_{4\bullet x}H_2O$ for anode materials in lithium-ion batteries with a high capacity, Ionics 26 (2020) 33–42.

[33] M.J. Aragon, B. Leon, V.C. Perez, J.L. Tirado, Synthesis and electrochemical reaction with lithium of mesoporous iron oxalate nanoribbons, J. Inorg. Chem. 47 (2018) 10366–10371.

[34] J.S. Yeoh, C.F. Armer, A. Lowe, Transition metal oxalates as energy storage materials. A review, Mater. Today Energy 9 (2018) 198–222.

[35] F.Y. Kong, X.D. He, Q.Q. Liu, X.X. Qi, D.D. Sun, Y.T. Zheng, et al., J. Electrochem. Commun. 97 (2018) 16–21.

[36] X. Guo, X.Q. Xie, S. Choi, Y.F. Zhao, H. Liu, C.Y. Wang, et al., Sb_2O_3/MXene (Ti_3C_2Tx) hybrid anode materials with enhanced performance for sodium-ion batteries, J. Mater. Chem. 5 (2013), 124445. -12452.

[37] F. Jiang, R. Du, X. Yan, M. Zhang, Q. Han, X. Sun, et al., Ferroferric oxide nanoclusters decorated Ti_3C_2Tx nanosheets as high performance anode materials for lithium ion batteries, J. Electrochim. Acta 29 (2020) 35146–35154.

[38] W. Ding, S. Wang, X. Wu, Y. Wang, Y. Li, P. Zhou, et al., $Co_{0.85}Se$@C/Ti_3C_2Tx MXene hybrids as anode materials for lithium-ion batteries, J. Alloy. Compd. 816 (2019) 152566–152605.

[39] M.W. Logan, D. Zhang, B. Tan, K. Gerasopoulos, A scalable aluminum niobate anode for high energy, high power practical lithium-ion batteries, J. Mater. Chem. A 9 (2021) 11228–11240.

[40] H. Aghamohammadi, R. Eslami-Farsani, E. Castillo-Martinez, Recent trends in the development of MXenes and MXene-based composites as anode materials for Li-ion batteries, J. Energy Storage (2021), 103572, https://doi.org/10.1016/j.est.2021.103572.

[41] X. Lou, R. Li, X. Zhu, L. Luo, Y. Chen, C. Lin, et al., New anode material for lithium-ion batteries: aluminum niobate ($AlNb_{11}O_{29}$), ACS Appl. Mater. Interface 11 (6) (2019) 6089–6096.

[42] X. Lu, Z. Jian, Z. Fang, L. Gu, Y.S. Hu, W. Chen, et al., Atomic scale investigation on lithium storagemechanism in $TiNb_2O_7$, J. Energy Environ. Sci. 4 (2011) 2638–2644.

[43] W. Liu, H. Zhi, X. Yu, Recent progress in phosphorus based anode materials for lithium/sodium ion batteries, J. Energy Storage Mater. 16 (2019) 290–322.

[44] H. Gao, F. Yang, Y. Zheng, Q. Zhang, J. Hao, S. Zhang, et al., Three-dimensionalporous cobalt phosphide nanocubes encapsulated in a graphene aerogel as an advanced anode with high coulombic efficiency for high-energy lithium-ion batteries, ACS Appl. Mater. Interfaces 11 (2019) 5373–5379.

[45] H. Wu, K. Wei, B. Tang, Y. Cui, Y. Zhao, M. Xue, et al., A novel Li_3P-VP nanocomposite fabricated by pulsed laser deposition as anode material for high-capacity lithium ion batteries, J. Electroanal. Chem. 841 (2019) 21–25.

[46] J. Wang, Y. Zhu, C. Zhang, F. Kong, S. Tao, B. Qian, et al., Bimetal phosphide $Ni_{1.4}Co_{0.6}P$ nanoparticle/carbon@ nitrogen-doped graphene network as high-performance anode materials for lithium-ion batteries, Appl. Surf. Sci. 485 (2019) 413–422.

[47] C.M. Doherty, R.A. Caruso, C.J. Drummond, High performance $LiFePO_4$ electrode materials: influence of colloidal particle morphology and porosity on lithium-ion battery power capability, Energy Environ. Sci. 3 (2010) 813.

[48] Z. Xing, Z.C. Ju, J. Yang, H.Y. Xu, Y.T. Qian, One-step hydrothermal synthesis of $ZnFe_2O_4$ nano-octahedrons as a high capacity anode material for Li-ion batteries, Nano Res. 5 (2012) 477.

[49] J. Liu, T.E. Conry, X.Y. Song, M.M. DoeffandT. J. Richardson, Nanoporous spherical $LiFePO_4$ for high performance cathodes, Energy Environ. Sci. 4 (2011) 885.

[50] P. Poizot, S. Laruelle, S. Grugeon, L. Dupontand, J.M. Tarascon, Nano-sized transition-metal oxides as negative-electrode materials for lithium-ion batteries, Nature 407 (2000) 496.

[51] Y. Deng, S.D. Tang, Q.M. Zhang, Z. Shi, L. Zhang, S. Zhanand, G.H. Chen, Controllable synthesis of spinel nano-$ZnMn_2O_4$via a single source precursor route and its high capacity retention as anode material for lithium ion batteries, J. Mater. Chem. 21 (2011) 11987.

[52] S.W. Kim, H.W. Lee, P. Muralidharan, D.H. Seo, W.S. Yoon, D.K. Kim, K. Kang, Electrochemical performance and *ex situ* analysis of $ZnMn_2O_4$ nanowires as anode materials for lithium rechargeable batteries, Nano Res. 4 (2011) 505–510.

[53] A. Vu, Y.Q. Qian, A. Stein, Porous electrode materials for lithium-ion batteries-how to prepare them and what makes them special, Adv. Energy Mater. 2 (2012) 1056.

[54] F.Y Cheng, H.B. Wang, Z.Q. Zhu, Y. Wang, T.R. Zhang, Z.L. Tao, J. Chen, Porous $LiMn_2O_4$ nanorods with durable high-rate capability for rechargeable Li-ion batteries, Energy Environ. Sci. 4 (2011) 3668.

[55] Z. Bai, N. Fan, C. Sun, Z. Ju, C. Guo, J. Yang, Y. Qian, Facile synthesis of loaf-like $ZnMn_2O_4$ nanorods and their excellent performance in Li-ion batteries, Nanoscale 5 (2013) 2442–2447.

[56] H. Aghamohammadi, N. Hassanzadeh, R. Eslami-Farsani, A review study on titanium niobium oxide-based composite anodes for Li-ion batteries: synthesis, structure, and performance, Ceram. Int. 47 (19) (2021) 26598–26619.

[57] C. Lin, G. Wang, S. Lin, J. Li, L. Lu, $TiNb_6O_{17}$: a new electrode material for lithium-ion batteries, Chem. Commun. 51 (2015) 8970–8973.

[58] K. Liu, J.A. Wang, J. Yang, D. Zhao, P. Chen, J. Man, X. Yu, Z. Wen, J. Sun, Interstitial and substitutional V5 -doped $TiNb_2O_7$ microspheres: a novel doping way to achieve high-performance electrode, Chem. Eng. J. 407 (2021), 127190.

[59] G. Zhu, Q. Li, Y. Zhao, R. Che, Nanoporous $TiNb_2O_7$/C composite microspherewith three-dimensional conductive network for long-cycle-life and

high-rate-capabilityanode materials for lithium-ion batteries, ACS Appl. Mater. Interfaces 9 (2017) 41258–41264.
[60] C. Lin, L. Hu, C. Cheng, K. Sun, X. Guo, Q. Shao, J. Li, N. Wang, Z. Guo, Nano-$TiNb_2O_7$/carbon nanotubes composite anode for enhanced lithium-ion storage, Electrochim. Acta 260 (2018) 65–72.
[61] Y. Yang, Y. Yue, L. Wang, X. Cheng, Y. Hu, Z.Z. Yang, R. Zhang, B. Jin, R. Sun, Facile synthesis of mesoporous $TiNb_2O_7$/C microspheres as long-life and high-power anodes for lithium-ion batteries, Int. J. Hydrog. Energy 45 (2020) 12583–12592.
[62] H. Li, Y. Zhang, Y. Tang, F. Zhao, B. Zhao, Y. Hu, H. Murat, S. Gao, L. Liu, $TiNb_2O_7$ nanowires with high electrochemical performances as anodes for lithiumion batteries, Appl. Surf. Sci. 475 (2019) 942–946.
[63] Y. Yang, Z. Li, R. Zhang, Y. Ding, H. Xie, G. Liu, Y. Fan, Z. Yang, X. Liu, Polydopamine-derived N-doped carbon-coated porous $TiNb_2O_7$ microspheres asanode materials with superior rate performance for lithium-ion batteries, Electrochim. Acta 368 (2021), 137623.
[64] C. Yuan, H.B. Wu, Y. Xie, X.W. Lou, Mixed Transition-metal oxides: design, synthesis, and energy-related applications, Angew. Chem. Int. Ed. 53 (2014) 1488.
[65] H. Jiang, T. Sun, C. Li, J. Ma, Hierarchical porous nanostructures assembled from ultrathin MnO_2nanoflakes with enhanced supercapacitive performances, J. Mater. Chem. 22 (2012) 2751.
[66] A. Pramanik, S. Maiti, S. Mahanty, Metal hydroxides as a conversion electrode forlithium-ion batteries: a case study with a $Cu(OH)_2$ nanoflower array, J. Nanosci. Lett. 5 (2015) 3.
[67] B. Li, H. Cao, J. Shao, H. Zheng, Y. Lu, J. Yin, M. Qu, Improved performances of β-$Ni(OH)_2$@reduced-graphene-oxide in Ni-MH and Li-ion batteries, Chem. Commun. 47 (2011) 3159.
[68] S. Ni, X. Lv, T. Li, X. Yang, L. Zhang, The investigation of $Ni(OH)_2$/Ni as anodes for high performance Li-ion batteries, J. Mater. Chem. A 1 (2013) 1544.
[69] X. Liu, R. Ma, Y. Bando, T. Sasaki, A general strategy to layered transition-metal hydroxide nanocones: tuning the composition for high electrochemical performance, Adv. Mater. 24 (2012) 2148.
[70] Y. Wang, S. Gai, N. Niu, F. He, P. Yang, Fabrication and electrochemical performance of 3D hierarchical β-$Ni(OH)_2$ hollow microspheres wrapped in reduced graphene oxide, J. Mater. Chem. A 1 (2013) 9083.
[71] H.B. Li, M.H. Yu, F.X. Wang, P. Liu, Y. Liang, J. Xiao, C.X. Wang, Y.X. Tong, G. W. Yang, Amorphous nickel hydroxide nanospheres with ultrahigh capacitance and energy density as electrochemical pseudocapacitor materials, Nat. Commun. 4 (2013) 1894.
[72] W. Zhang, X. Wen, S. Yang, Y. Berta, L. Wang, Single-crystalline scroll-type nanotube arrays of copper hydroxide synthesized at room temperature, Adv. Mater. 15 (2003) 822.
[73] P. Gao, M. Zhang, Z. Niu, Q. Xiao, A facile solution-chemistry method for Cu $(OH)_2$ nanoribbon arrays with noticeable electrochemical hydrogen storage ability at room temperature, Chem. Commun. (2007) 5197.
[74] A. Pramanik, S. Maiti, S. Mahanty, Metal hydroxides as a conversion electrode for lithium-ion batteries: a case study with a $Cu(OH)_2$ nanoflower array, J. Mater. Chem. A 2 (2014) 18515.
[75] J. Cabana, L. Monconduit, D. Larcher, M.R. Palacín, Beyond intercalation-based Li-ion batteries: the state of the art and challenges of electrode materials reacting through conversion reactions, Adv. Mater. 22 (2010) E170.
[76] P.G. Bruce, S.A. Freunberger, L.J. Hardwick, J.M. Tarascon, Li–O_2 and Li–S batteries with high energy storage, Nat. Mater. 11 (2012) 19.
[77] W. Dreyer, J. Jamnik, C. Guhlke, R. Huth, J. Moskon, M. Gaberscek, The thermodynamic origin of hysteresis in insertion batteries, Nat. Mater. 9 (2010) 448.
[78] L. Li, R. Jacobs, P. Gao, L. Gan, F. Wang, D. Morgan, S. Jin, Origins of large voltage hysteresis in high-energy-density metal fluoride lithium-ion battery conversion electrodes, J. Am. Chem. Soc. 138 (2016) 2838–2848.
[79] R.E. Doe, K.A. Persson, Y.S. Meng, G. Ceder, First-principles investigation of the Li−Fe−F phase diagram and equilibrium and nonequilibrium conversion reactions of iron fluorides with lithium, Chem. Mater. 20 (2008) 5274.
[80] P. Liu, J.J. Vajo, J.S. Wang, W.J.L. Li, Thermodynamics and kinetics of the Li/FeF_3 reaction by electrochemical analysis, J. Phys. Chem. C 116 (2012) 6467.
[81] J.K. Ko, M.K. Wiaderek, N. Pereira, T.L. Kinnibrugh, J.R. Kim, P.J. Chupas, K. W. Chapman, G.G. Amatucci, Transport, phase reactions, and hysteresis of iron fluoride and oxyfluoride conversion electrode materials for lithium batteries, ACS Appl. Mater. Interfaces 6 (2014) 10858.
[82] F. Wang, J. Yi, Y. Wang, C. Wang, J. Wang, Y. Xia, Graphite intercalation compounds (GICs): a new type of promising anode material for lithium-ion batteries, Adv. Energy Mater. 4 (2014), 1300600.
[83] F. Wang, S.W. Kim, D.H. Seo, K. Kang, L. Wang, D. Su, J.J. Vajo, J. Wang, J. Graetz, Ternary metal fluorides as high-energy cathodes with low cycling hysteresis, Nat. Commun. 6 (2015) 6668.
[84] X. Hua, R. Robert, L.S. Du, K.M. Wiaderek, M. Leskes, K.W. Chapman, P. J. Chupas, C.P. Grey, Comprehensive study of the CuF_2 conversion reaction mechanism in a lithium ion battery, J. Phys. Chem. C 118 (2014) 15169.
[85] X. Li, F.E. Kersey-Bronec, J. Ke, J.E. Cloud, Y. Wang, C. Ngo, S. Pylypenko, Y. Yang, Study of lithium silicide nanoparticles as anode materials for advanced lithium ion batteries, ACS Appl. Mater. Interfaces 9 (2017) 16071–16080.
[86] M. Raić, L. Mikac, I. Marić, G. Štefanić, M. Škrabić, M. Gotić, M. Ivanda, Nanostructured silicon as potential anode material for Li-ion batteries, Molecules 25 (4) (2020) 891.
[87] M.N. Obrovac, L. Christensen, Structural changes in silicon anodes during lithium insertion/extraction, J. Electrochem. Solid-State Lett. 7 (2004) A93–A96.
[88] Y. Jin, B. Zhu, Z. Lu, N. Liu, J. Zhu, Challenges and recent progress in the development of Si anodes for lithium-ion battery, Adv. Energy Mater. 7 (2017), 1700715.
[89] J.H. Ryu, J.W. Kim, Y.E. Sung, S.M. Oh, Failure modes of silicon powder negative electrode in lithium secondary batteries, Electrochem. Solid State Lett. 7 (2004) A306–A309.
[90] M. Ge, X. Fang, J. Rong, C. Zhou, Review of porous silicon preparation and its application for lithium-ion battery anodes, Nanotechnology 24 (2013), 422001.
[91] H. Yang, H. Bang, K. Amine, J. Prakash, Investigations of the exothermic reactions of natural graphite anode for Li-ion batteries during thermal runaway, J. Electrochem. Soc. 152 (2005) A73–A79.
[92] M.D. Levi, D. Aurbach, Simultaneous measurements and modeling of the electrochemical impedance and the cyclic voltammetric characteristics of graphite electrodes doped with lithium, J. Phys. Chem. B 101 (1997) 4641–4647.
[93] K. Persson, V.A. Sethuraman, L.J. Hardwick, Y. Hinuma, Y.S. Meng, A. van der Ven, V. Srinivasan, R. Kostecki, G. Ceder, Lithium diffusion in graphitic carbon, J. Phys. Chem. Lett. 1 (2010) 1176–1180.
[94] M.K. Jangid, F.J. Sonia, R. Kali, B. Ananthoju, A. Mukhopadhyay, Insights into the effects of multi-layered graphene as buffer/interlayer for a-Si during lithiation/delithiation, Carbon 111 (2017) 602–616.
[95] M.K. Jangid, A. Mukhopadhyay, Real-time monitoring of stress development during electrochemical cycling of electrode materials for Li-ion batteries: overview and perspectives, J. Mater. Chem. A7 (2019) 23679–23726.
[96] N. Ding, J. Xu, Y.X. Yao, G. Wegner, X. Fang, C.H. Chen, I. Lieberwirth, Determination of the diffusion coefficient of lithium ions in nano-Si, Solid State Ion. 180 (2009) 222–225.
[97] M. Pharr, K. Zhao, X. Wang, Z. Suo, J.J. Vlassak, Kinetics of initial lithiation of crystalline silicon electrodes of lithium-ion batteries, Nano Lett. 12 (2012) 5039–5047.
[98] N.A. Kaskhedikar, J. Maier, Lithium storage in carbon nanostructures, Adv. Mater. 21 (2009) 2664–2680.
[99] M.K. Jangid, A. Mukhopadhyay, Silicon based anode materials for Li-ion batteries – importance, challenges and strategies, SMC Bull. 10 (3) (2019) 167–178.
[100] T.D. Hatchard, J.R. Dahn, *In situ* XRD and electrochemical study of the reaction of lithium with amorphous silicon, J. Electrochem. Soc. 151 (2004) A838–A842.
[101] W. Ren, Z. Zhang, Y. Wang, Q. Tan, Z. Zhong, F. Su, Preparation of porous silicon/carbon microspheres as high performance anode materials for lithium ion batteries, J. Mater. Chem. A 3 (2015) 5859–5865.
[102] S.J.L. Billinge, I. Levin, The problem with determining atomic structure at the nanoscale, Science 316 (2007) 561–565.
[103] V. Petkov, B. Prasai, Y. Ren, S. Shan, J. Luo, P. Joseph, C.J. Zhong, Solving the nanostructure problem: exemplified on metallic alloy nanoparticles, Nanoscale 6 (2014) 10048–10061.
[104] A.S. Arico, P. Bruce, B. Scrosati, J.M. Tarascon, W. van Schalk, Nanostructured materials for advanced energy conversion and storage devices, J. Nat. Mater. 4 (2005) 366–377.
[105] B. Hertzberg, A. Alexeev, G. Yushin, Deformations in Si-Li anodes upon electrochemical alloying in nano-confined space, J. Am. Chem. Soc. 132 (25) (2010) 8548–8549.
[106] H. Wu, G. Zheng, N. Liu, T.J. Carney, Y. Yang, Y. Cui, Engineering empty space between Si nanoparticles for lithium-ion battery anodes, J. Nano Lett. 12 (2012) 904–909.
[107] J. Ji, H. Ji, L.L. Zhang, X. Zhao, X. Bai, X. Fan, F. Zhang, R.S. Ruo, Graphene-encapsulated Si on ultrathin-graphite foam as anode for high capacity lithium-ion batteries, Adv. Mater. 25 (2013) 4673–4677.
[108] N. Liu, Z. Lu, J. Zhao, M.T. McDowell, H.W. Lee, W. Zhao, Y. Cui, A pomegranate-inspired nanoscale design for large-volume-change lithium battery anodes, Nat. Nanotechnol. 9 (2014) 187–192.
[109] M.K. Wang, L. Qi, F. Zhao, S.J. Dong, A novel comb-like copolymer based polymer electrolyte for Li batteries, J. Power Sources 139 (2005) 223.
[110] B. Philippe, R. Dedryvere, J. Allouche, F. Lindgren, M. Gorgoi, H. Rensmo, D. Gonbeau, K. Edstrom, Nanosilicon electrodes for lithium-ion batteries: interfacial mechanisms studied by hard and soft X-ray photoelectron spectroscopy, Chem. Mater. 24 (2012) 1107.
[111] L. Pan, H.B. Wang, D.C. Gao, S.Y. Chen, L. Tan, L. Li, Facile synthesis of yolk–shell structured Si–C nanocomposites as anodes for lithium-ion batteries, Chem. Commun. 50 (2014) 5878.
[112] G.B. Han, M.H. Ryou, K.Y. Cho, Y.M. Lee, J.K. Park, Effect of succinic anhydride as an electrolyte additive on electrochemical characteristics of silicon thin-film electrode, J. Power Sources 195 (2010) 3709.
[113] S.Y. Li, B.C. Li, X.L. Xu, X.M. Shi, Y.Y. Zhao, L.P. Mao, X.L. Cui, Electrochemical performances of two kinds of electrolytes based on lithium bis(oxalate)borate and sulfolane for advanced lithium ion batteries, J. Power Sources 209 (2012) 295.
[114] S. Dalavi, P. Guduru, B.L. Lucht, Performance enhancing electrolyte additives for lithium ion batteries with silicon anodes, J. Electrochem. Soc. 159 (2012) A642.
[115] L.B. Chen, K. Wang, X.H. Xie, J.Y. Xie, Effect of vinylene carbonate (VC) as electrolyte additive on electrochemical performance of Si film anode for lithium ion batteries, J. Power Sources 174 (2007) 538.
[116] V. Etacheri, O. Haik, Y. Goffer, G.A. Roberts, I.C. Stefan, R. Fasching, D. Aurbach, Effect of fluoroethylene carbonate (FEC) on the performance and surface chemistry of Si-nanowire Li-ion battery anodes, Langmuir 28 (2012) 965–976.
[117] M. Gauthier, T.J. Carney, A. Grimaud, L. Giordano, N. Pour, H.H. Chang, D. P. Fenning, S.F. Lux, O. Paschos, C. Bauer, F. Magia, S. Lupart, P. Lamp, Y. Shao-Horn, Electrode-electrolyte interface in Li-ion batteries: current understanding and new insights, J. Phys. Chem. Lett. 6 (2015) 4653.

[118] K. Xu, Electrolytes and interphases in Li-ion batteries and beyond, Chem. Rev. 114 (2014) 11503–11618.
[119] H. Ota, Y. Sakata, A. Inoue, S. Yamaguchi, Analysis of vinylene carbonate derived SEI layers on graphite anode, J. Electrochem. Soc. 151 (2004) A1659.
[120] H. Nakai, T. Kubota, A. Kita, A. Kawashima, Investigation of the solid electrolyte interphase formed by fluoroethylene carbonate on Si electrodes, J. Electrochem. Soc. 158 (2011) A798.
[121] C. Xu, F. Lindgren, B. Philippe, M. Gorgoi, F. Bjorefors, K. Edstrom, T. Gustafsson, Improved performance of the silicon anode for Li-ion batteries: understanding the surface modification mechanism of fluoroethylene carbonate as an effective electrolyte additive, Chem. Mater. 27 (2015) 2591.
[122] S. Malmgren, K. Ciosek, M. Hahlin, T. Gustafsson, M. Gorgoi, H. Rensmo, K. Edstrom, Comparing anode and cathode electrode/electrolyte interface composition and morphology using soft and hard X-ray photoelectron spectroscopy, Electrochem. Acta 97 (2013) 23.
[123] M. Zhao, Y. Xia, X. Liu, Z. Tan, B. Huang, F. Li, Y. Ji andC. Song, Curvature-induced condensation of lithium confined inside single-walled carbon nanotubes: First-principles calculations, Phys. Lett. A 340 (2005) 434–439.
[124] B.J. Landi, M.J. Ganter, C.M. Schauerman, C.D. Cressand, A.R.P. Rachaelle, Lithium ion capacity of single wall carbon nanotube paper electrodes, J. Phys. Chem. C 112 (19) (2008) 7509–7515.
[125] B. Ribeiro, E.C. Botelho, M.L. Costa, C.F. Bandeira, Polimeros 27 (2017) 104–142.
[126] L. Guadagno, M. Raimondo, V. Vittoria, L. Vertuccio, K. Lafdi, B. De Vivo, P. Lamberti, G. Spinelli, V. Tucci, The role of carbon nanofiber defects on the electrical and mechanical properties of CNF-based resins, Nanotechnology 24 (2013) 305704–305714.
[127] S. Tigges, N. Wöhrl, U. Hagemann, M. Ney, A. Lorke, The effect of metal-oxide incorporation on the morphology of carbon nanostructures, J. Phys. D Appl. Phys. 53 (2020) 145206–145220.
[128] A. Magasinski, P. Dixon, B. Hertzberg, A. Kvit, J. Ayala, G. Yushin, High-performance lithium-ion anodes using a hierarchical bottom-up approach, Nat. Mater. 9 (2010) 353–358.
[129] H. Xiang, Z. Li, K. Xie, J. Jiang, J. Chen, P. Lian, J. Wu, Y. Yu, H. Wang, Graphene sheets as anode materials for Li-ion batteries: preparation, structure, electrochemical properties and mechanism for lithium storage, RSC Adv. 2 (2012) 6792–6799.
[130] M. Srivastava, J. Singh, T. Kuila, R.K. Layek, N.H. Kim, J.H. Lee, Recent advances in graphene and its metal-oxide hybrid nanostructures for lithium-ion batteries, Nanoscale 7 (2015) 4820–4868.
[131] X. Ji, Y. Mu, J. Liang, T. Jiang, J. Zeng, Z. Lin, Y. Lin, J. Yu, High yield production of 3D graphene powders by thermal chemical vapor deposition and application as highly efficient conductive additive of lithium ion battery electrodes, Carbon 176 (2021) 21–30.
[132] H. Aghamohammadi, N. Hassanzadeh, R. Eslami-Farsani, A review study on the recent advances in developing the heteroatom-doped graphene and porous graphene as superior anode materials for Li-ion batteries, Ceram. Int. 47 (16) (2021) 22269–22301.
[133] H. Aghamohammadi, R. Eslami-Farsani, M. Torabian, N. Amousa, Recent advances in one-pot functionalization of graphene using electrochemical exfoliation of graphite: a review study, Synth. Met. 269 (2020), 116549.
[134] S.H. Abbandanak, H. Aghamohammadi, E. Akbarzadeh, N. Shabani, R. Eslami-Farsani, M. Kangooie, M.H. Siadati, Morphological/SAXS/WAXS studies on the electrochemical synthesis of graphene nanoplatelets, Ceram. Int. 45 (2019) 20882–20890.
[135] P. Shi, J. Guo, X. Liang, S. Cheng, H. Zheng, Y. Wang, C. Chen, H. Xiang, Large-scale production of high-quality graphene sheets by a non-electrified electrochemical exfoliation method, Carbon 126 (2018) 507–513.
[136] H. Gürsu, Y. Güner, K.B. Dermenci, M. Gençten, A.F. Buluç, U. Savacı, S. Turan, Y. Sahin, Preparation of N-doped graphene powders by cyclic voltammetry and a potential application of them: anode materials of Li-ion batteries, Int. J. Energy Res. 43 (2019) 5346–5354.
[137] A. Lokhande, I. Qattan, C. Lokhande, S.P. Patole, Holey graphene: an emerging versatile material, J. Mater. Chem. 8 (2020) 918–977.
[138] Y. Zhang, Q. Wan, N. Yang, Recent advances of porous graphene: synthesis, functionalization, and electrochemical applications, Small 15 (2019), 1903780.
[139] A. Guirguis, J.W. Maina, X. Zhang, L.C. Henderson, L. Kong, H. Shon, L.F. Dumée, Applications of nano-porous graphene materials–critical review on performance and challenges, Mater. Horiz. 7 (2020) 1218–1245.
[140] T. Liu, L. Zhang, B. Cheng, X. Hu, J. Yu, Holey graphene for electrochemical energy storage, Cell Rep. Phys. Sci. (2020), 100215.
[141] H. Cao, X. Zhou, C. Zheng, Z. Liu, Metal etching method for preparing porous graphene as high performance anode material for lithium-ion batteries, Carbon 89 (2015) 41–46.
[142] M.W. Roberts, C.B. Clemons, J.P. Wilber, G.W. Young, A. Buldum, D.D. Quinn, Continuum plate theory and atomistic modeling to find the flexural rigidity of a graphene sheet interacting with a substrate, J. Nanotechnol. (2010). Article ID 868492.
[143] S. Nardecchia, D. Carriazo, M.L. Ferrer, M.C. Gutierrez, F. del Monte, Three dimensional macroporous architectures and aerogels built of carbon nanotubes and/or graphene: synthesis and applications, Chem. Soc. Rev. 42 (2013) 794–830.
[144] Y.Z. Jin, C. Gao, W.K. Hsu, Y. Zhu, A. Huczko, M. Bystrzejewski, M. Roe, C.Y. Lee, S. Acquah, H. Krotoand, D.R.M. Walton, Large-scale synthesis and characterization of carbon spheres prepared by direct pyrolysis of hydrocarbons, Carbon 43 (2005) 1944–1953.